The Journal of Chemical Physics

Theory, implementation, and disappointing results for two-photon absorption cross sections within the doubly electron-attached equation-of-motion coupled-cluster framework

Cite as: J. Chem. Phys. **158**, 054102 (2023); https://doi.org/10.1063/5.0135052
Submitted: 16 November 2022 • Accepted: 29 December 2022 • Accepted Manuscript Online: 02 January 2023 • Published Online: 02 February 2023

Kaushik D. Nanda, Sahil Gulania and Anna I. Krylov

The Journal of Chemical Physics ARTICLE scitation.org/journal/jcp

Theory, implementation, and disappointing results for two-photon absorption cross sections within the doubly electron-attached equation-of-motion coupled-cluster framework

Cite as: J. Chem. Phys. 158, 054102 (2023); doi: 10.1063/5.0135052
Submitted: 16 November 2022 • Accepted: 29 December 2022 •
Published Online: 2 February 2023

Kaushik D. Nanda,[a] Sahil Gulania, and Anna I. Krylov[b]

AFFILIATIONS

Department of Chemistry, University of Southern California, Los Angeles, California 90089-0482, USA

[a]Author to whom any correspondence should be addressed: kaushikdnanda@gmail.com
[b]Electronic mail: krylov@usc.edu

ABSTRACT

The equation-of-motion coupled-cluster singles and doubles method with double electron attachment (EOM-DEA-CCSD) is capable of computing reliable energies, wave functions, and first-order properties of excited states in diradicals and polyenes that have a significant doubly excited character with respect to the ground state, without the need for including the computationally expensive triple excitations. Here, we extend the capabilities of the EOM-DEA-CCSD method to the calculations of a multiphoton property, two-photon absorption (2PA) cross sections. Closed-form expressions for the 2PA cross sections are derived within the expectation-value approach using response wave functions. We analyze the performance of this new implementation by comparing the EOM-DEA-CCSD energies and 2PA cross sections with those computed using the CC3 quadratic response theory approach. As benchmark systems, we consider transitions to the states with doubly excited character in twisted ethene and in polyenes, for which EOM-EE-CCSD (EOM-CCSD for excitation energies) performs poorly. The EOM-DEA-CCSD 2PA cross sections are comparable with the CC3 results for twisted ethene; however, the discrepancies between the two methods are large for hexatriene. The observed trends are explained by configurational analysis of the 2PA channels.

I. INTRODUCTION

Molecular photoswitches have seen increasing interest in applications as varied as optical limiting, optogenetics, molecular optoelectronics, and photopharmacology.[1–7] In many of these applications, the function of photoswitches is controlled through their nonlinear response to light. *A priori* understanding of these nonlinear response properties through theoretical modeling can, therefore, facilitate the design of functional photoswitches.

One class of photoswitching behavior is based on the *cis–trans* isomerization of conjugated chromophores, such as molecules with polyene backbone. Such photoswitching commonly occurs in biological systems, e.g., the initial step in vision is the *cis*-to-*trans* photoisomerization of the retinal.[8] The switching process in such systems proceeds via open-shell structures with diradical character. The theoretical treatment of diradical electronic structure requires sophisticated methods that can provide a balanced treatment of static and dynamical electronic correlation. Furthermore, accurate modeling of the excitation-energy spectra of prototypical polyenes (e.g., *trans*-butadiene, *trans*-hexatriene, and *trans*-octatetraene) is notoriously difficult due to the presence of low-lying states with doubly excited character.[9–17] For example, the $2A_g$ singlet in *trans*-butadiene has contributions from both the Rydberg excitations and doubly excited configurations relative to its ground state, which requires methods that can describe these contributions in a balanced fashion.

A few strategies, such as the semistochastic heat-bath configuration interaction,[16] the incremental full configuration interaction,[18,19] and the equation-of-motion coupled-cluster methods for electronic excitations[15] (EOM-EE-CC), have been reported to be able to reliably describe the low-lying excited states in prototypical polyenes. In particular, the EOM-CC hierarchy of methods

provides a robust single-reference, multi-state framework for systematically improvable benchmark results through the inclusion of higher-order excited determinants (singles, doubles, triples, quadruples, and so on).[20–30] The single-reference, multi-state feature of the EOM-CC framework is particularly attractive for modeling spectra that require the calculation of multiple states from the same model Hamiltonian. However, the steep increase in the computational cost for these series of methods limits the applicability of the high-level EOM-CC methods (e.g., EOM-CCSDT, EOM-CCSDTQ, etc.) to small systems.

In contrast to the standard EOM-CC hierarchy built upon the ground-state reference, low-lying states of systems with diradical character can be described by spin-flipping[26,31,32] and particle non-conserving EOM-CC treatments.[27,33–35] In particular, the EOM-CC singles and doubles method for doubly electron-attached states[34–39] (EOM-DEA-CCSD) describes the target states of diradicals or polyenes by attaching two electrons to the dicationic reference, which is well described by the Hartree–Fock determinant. The resulting space of the doubly electron-attached determinants ($2p$ and $3p1h$ with respect to the dicationic reference) provides a balanced description of singly and doubly excited configurations from the HOMO (highest occupied molecular orbital) with respect to the ground-state (neutral) reference. The EOM-DEA-CCSD ($2p + 3p1h$) approach has been shown to provide reliable energies for excited states that otherwise require higher-level EOM-CC methods such as EOM-EE-CCSDT.[34,35,37–39]

In this paper, we extend the analysis of the EOM-DEA-CCSD method and its domain of applicability beyond excitation energies and first-order properties to compute two-photon absorption (2PA) cross sections for transitions in prototypical polyenes. As for other nonlinear optical properties, the observable is given in terms of 2PA moments that are formally expressed using sum-over-all-states (SOS) expressions. Here, we explain how these SOS expressions are converted into compact expectation-value-like expressions using the first-order response wave functions of the EOM-DEA-CCSD target states. We benchmark the 2PA cross sections for transitions in twisted ethene and polyenes computed within the EOM-DEA-CCSD framework against those computed with the higher-level CC3 quadratic response theory.[40–43] We rationalize the quality of EOM-DEA-CCSD results using the uncorrelated picture of the 2PA configurational channels. We illustrate the much stronger sensitivity of 2PA cross sections, compared to energies and first-order properties, to the electronic correlation and the configuration space spanned by the model Hamiltonian.

II. THEORY

A. CCSD and EOM-DEA-CCSD theory

The CCSD wave function[44–48] is expressed as

$$\Psi = e^{\hat{T}}|\Phi_0\rangle, \tag{1}$$

where Φ_0 is the reference Slater determinant (usually the Hartree–Fock solution). For example, a typical reference determinant in the EOM-DEA-CCSD method is the Hartree–Fock determinant of the dicationic system.[39] $\hat{T}$ is the cluster operator satisfying the CCSD equations,

$$\langle\Phi_\nu|\hat{\bar{H}}|\Phi_0\rangle = 0, \tag{2}$$

where ν spans the singles and doubles excitation manifold and $\hat{\bar{H}} = e^{-\hat{T}}\hat{H}e^{\hat{T}}$ is the similarity-transformed Hamiltonian. $\hat{T}$ is expressed in terms of the electron-creation ($\hat{a}^\dagger$ and $\hat{b}^\dagger$) and electron-annihilation operators ($\hat{i}$ and $\hat{j}$) as follows:

$$\begin{aligned}\hat{T} &= \hat{T}_1 + \hat{T}_2;\\ \hat{T}_1 &= \sum_{ia} t_i^a \hat{a}^\dagger \hat{i};\\ \hat{T}_2 &= \frac{1}{4}\sum_{ijab} t_{ij}^{ab} \hat{a}^\dagger \hat{b}^\dagger \hat{j}\hat{i}.\end{aligned} \tag{3}$$

The right and left EOM-DEA-CCSD wave functions and energy (E^k) for the k^{th} target state are defined by the right (electron-attachment) and left (electron-detachment) EOM-DEA-CCSD operators, $\hat{R}^k$ and $\hat{L}^k$, satisfying the following eigenvalue equations:[21,24,27,39]

$$\hat{\bar{H}}\hat{R}^k|\Phi_0\rangle = E^k\hat{R}^k|\Phi_0\rangle \tag{4}$$

and

$$\langle\Phi_0|\hat{L}^k\hat{\bar{H}} = \langle\Phi_0|\hat{L}^k E^k, \tag{5}$$

where $\hat{R}^k$ and $\hat{L}^k$ are given by

$$\begin{aligned}\hat{R}^k &= \hat{R}_1^k + \hat{R}_2^k,\\ \hat{R}_1 &= \frac{1}{2}\sum_{ab} r^{ab}\hat{a}^\dagger\hat{b}^\dagger,\\ \hat{R}_2 &= \frac{1}{6}\sum_{iabc} r_i^{abc}\hat{a}^\dagger\hat{b}^\dagger\hat{c}^\dagger\hat{i}\end{aligned} \tag{6}$$

and

$$\begin{aligned}\hat{L}^k &= \hat{L}_1^k + \hat{L}_2^k,\\ \hat{L}_1 &= \frac{1}{2}\sum_{ab} l^{ab}\hat{a}^\dagger\hat{b}^\dagger,\\ \hat{L}_2 &= \frac{1}{6}\sum_{iabc} l_i^{abc}\hat{a}^\dagger\hat{b}^\dagger\hat{c}^\dagger\hat{i}.\end{aligned} \tag{7}$$

In the amplitudes in Eqs. (3), (6), and (7), the labels i and j represent occupied (O) spin orbitals and a, b, and c represent virtual (V) spin orbitals, with respect to the reference determinant Φ_0. Thus, the EOM-DEA-CCSD $\hat{R}$ and $\hat{L}$ are given in terms of operators of the types VV ($2p$) and $OVVV$ ($1h3p$).

B. 2PA cross sections for transitions between EOM-DEA-CCSD states

For parallel linearly polarized light, the microscopic cross sections (δ^{fg}) for 2P transitions between the initial (g) and final (f) states are expressed in terms of the elements of the 2PA strength tensor (S_{wxyz}^{fg}) according to Refs. 43 and 49,

$$\delta^{fg} = \frac{1}{15}\sum_{x,y} S_{xxyy}^{fg} + \frac{1}{15}\sum_{x,y} S_{xyxy}^{fg} + \frac{1}{15}\sum_{x,y} S_{xyyx}^{fg}, \tag{8}$$

where w, x, y, and z span the Cartesian components. S_{wxyz}^{fg} are expressed in terms of the elements of the left and right 2PA transition-moment tensors, $M^{f\leftarrow g}$ and $M^{g\leftarrow f}$, respectively, as follows:

$$S_{wxyz}^{fg} = \frac{1}{2}\left(M_{wx}^{g\leftarrow f}M_{yz}^{f\leftarrow g} + \left(M_{yz}^{g\leftarrow f}\right)^*\left(M_{wx}^{f\leftarrow g}\right)^*\right). \tag{9}$$

Within CC response theory, properties are formulated as derivatives of appropriate (quasi)energy Lagrangians with respect to the strength of the external perturbation(s).[50–52] The 2PA moments can be computed as the first residues of the ground-state quadratic response function (first electric-dipole hyperpolarizability tensor) or, alternatively, the 2PA strength tensor elements can be computed as first residues of the ground-state cubic response function (second electric-dipole hyperpolarizability tensor). Compared to the residues of response functions, 2PA moments are more efficiently computed as second derivatives of appropriate transition-moment Lagrangians within CC response theory.[50,53]

Instead of CC response theory, we employ the EOM-CC expectation-value approach[49,54–58] in which the expressions for 2PA moments for exact wave functions are parameterized using EOM-CC wave functions and energies (E^k). The 2PA moments for exact wave functions (Ψ_ks) are expressed according to the following SOS expressions:

$$M_{yz}^{f\leftarrow g} = -\sum_n \frac{\langle \Psi^f|\hat{\mu}_z|\Psi^n\rangle\langle\Psi^n|\hat{\mu}_y|\Psi^g\rangle}{\mathcal{E}^n - \mathcal{E}^g - \omega_1} - \sum_n \frac{\langle \Psi^f|\hat{\mu}_y|\Psi^n\rangle\langle\Psi^n|\hat{\mu}_z|\Psi^g\rangle}{\mathcal{E}^n - \mathcal{E}^g - \omega_2} \tag{10}$$

and

$$M_{yz}^{g\leftarrow f} = -\sum_n \frac{\langle \Psi^g|\hat{\mu}_y|\Psi^n\rangle\langle\Psi^n|\hat{\mu}_z|\Psi^f\rangle}{\mathcal{E}^n - \mathcal{E}^g - \omega_1} - \sum_n \frac{\langle \Psi^g|\hat{\mu}_z|\Psi^n\rangle\langle\Psi^n|\hat{\mu}_y|\Psi^f\rangle}{\mathcal{E}^n - \mathcal{E}^g - \omega_2}, \tag{11}$$

where $\hat{\mu}$ is the dipole-moment operator, $\mathcal{E}^k$ is the energy of state k, and ω_1 and ω_2 are the energies of the absorbed photons polarized along the y and z directions, respectively. The absorbed photon energies satisfy the 2PA resonance condition: $\omega_1 + \omega_2 = \mathcal{E}^f - \mathcal{E}^g$. Within the expectation-value framework, the EOM-CC-parameterized Eqs. (10) and (11) are given by

$$M_{yz}^{f\leftarrow g} = -\sum_n \frac{\langle\Phi_0|\hat{L}^f\hat{\bar{\mu}}_z\hat{R}^n|\Phi_0\rangle\langle\Phi_0|\hat{L}^n\hat{\bar{\mu}}_y\hat{R}^g|\Phi_0\rangle}{E^n - E^g - \omega_1} - \sum_n \frac{\langle\Phi_0|\hat{L}^f\hat{\bar{\mu}}_y\hat{R}^n|\Phi_0\rangle\langle\Phi_0|\hat{L}^n\hat{\bar{\mu}}_z\hat{R}^g|\Phi_0\rangle}{E^n - E^g - \omega_2} \tag{12}$$

and

$$M_{yz}^{g\leftarrow f} = -\sum_n \frac{\langle\Phi_0|\hat{L}^g\hat{\bar{\mu}}_y\hat{R}^n|\Phi_0\rangle\langle\Psi_0|\hat{L}^n\hat{\bar{\mu}}_z\hat{R}^f|\Phi_0\rangle}{E^n - E^g - \omega_1} - \sum_n \frac{\langle\Phi_0|\hat{L}^g\hat{\bar{\mu}}_z\hat{R}^n|\Phi_0\rangle\langle\Phi_0|\hat{L}^n\hat{\bar{\mu}}_y\hat{R}^f|\Phi_0\rangle}{E^n - E^g - \omega_2}, \tag{13}$$

respectively, where $\hat{\bar{\mu}}_y = e^{-\hat{T}}\hat{\mu}_y e^{\hat{T}}$ is the similarity-transformed dipole-moment operator and $\omega_1 + \omega_2 = E^f - E^g$. Compared to the EOM-CC expectation-value approach, additional response intermediates are required within the CC response theory. The EOM-CC expectation-value parameterization also avoids artificial poles that spoil the pole structure of frequency-dependent properties computed within the CC response theory framework.[55]

The SOS expressions in Eqs. (12) and (13) are impractical for actual calculations as they entail the calculation of *all* states of the system. However, as explained below, they can be reformulated into closed-form expressions using response wave functions, providing a robust and practical strategy for computing 2PA moments.

Introducing the identity operator, $\hat{\mathbf{1}} = \sum_\rho |\Phi_\rho\rangle\langle\Phi_\rho|$ in Eqs. (12) and (13), we obtain

$$M_{yz}^{f\leftarrow g} = -\sum_{\rho\nu}\langle\Phi_0|\hat{L}^f\hat{\bar{\mu}}_z|\Phi_\rho\rangle\sum_n \frac{\langle\Phi_\rho|\hat{R}^n|\Phi_0\rangle\langle\Phi_0|\hat{L}^n|\Phi_\nu\rangle}{E^n - E^g - \omega_1}\langle\Phi_\nu|\hat{\bar{\mu}}_y\hat{R}^g|\Phi_0\rangle - \sum_{\rho\nu}\langle\Phi_0|\hat{L}^f\hat{\bar{\mu}}_y|\Phi_\rho\rangle\sum_n \frac{\langle\Phi_\rho|\hat{R}^n|\Phi_0\rangle\langle\Phi_0|\hat{L}^n|\Phi_\nu\rangle}{E^n - E^g - \omega_2}\langle\Phi_\nu|\hat{\bar{\mu}}_z\hat{R}^g|\Phi_0\rangle \tag{14}$$

and

$$M_{ab}^{g\leftarrow f} = -\sum_{\rho\nu}\langle\Phi_0|\hat{L}^g\hat{\bar{\mu}}_y|\Phi_\rho\rangle\sum_n \frac{\langle\Phi_\rho|\hat{R}^n|\Phi_0\rangle\langle\Phi_0|\hat{L}^n|\Phi_\nu\rangle}{E^n - E^g - \omega_1}\langle\Phi_\nu|\hat{\bar{\mu}}_z\hat{R}^f|\Phi_0\rangle - \sum_{\rho\nu}\langle\Phi_0|\hat{L}^g\hat{\bar{\mu}}_z|\Phi_\rho\rangle\sum_n \frac{\langle\Phi_\rho|\hat{R}^n|\Phi_0\rangle\langle\Phi_0|\hat{L}^n|\Phi_\nu\rangle}{E^n - E^g - \omega_2}\langle\Phi_\nu|\hat{\bar{\mu}}_y\hat{R}^f|\Phi_0\rangle, \tag{15}$$

respectively, where ρ and ν span the full configuration space. For the EOM-DEA-CCSD, however, only the terms with ρ and ν spanning the EOM-DEA-CCSD configuration space survive. Using first-order response wave functions ($X^k_{y,\omega}$ and $\tilde{X}^k_{y,\omega}$), Eqs. (14) and (15) can be recast in compact closed-form expressions as follows:[49]

$$\begin{aligned} M_{yz}^{f\leftarrow g} &= -\langle\Phi_0|\hat{L}^f\hat{\bar{\mu}}_z|X^g_{y,\omega_1}\rangle - \langle\Phi_0|\hat{L}^f\hat{\bar{\mu}}_y|X^g_{z,\omega_2}\rangle \\ &= -\sum_\rho \left[\tilde{D}^f_z\right]_\rho\left[X^g_{y,\omega_1}\right]_\rho - \sum_\rho\left[\tilde{D}^f_y\right]_\rho\left[X^g_{z,\omega_2}\right]_\rho \end{aligned} \tag{16}$$

and

$$\begin{aligned} M_{yz}^{g\leftarrow f} &= -\langle\tilde{X}^g_{y,\omega_1}|\hat{\bar{\mu}}_z\hat{R}^f|\Phi_0\rangle - \langle\tilde{X}^g_{z,\omega_2}|\hat{\bar{\mu}}_y\hat{R}^f|\Phi_0\rangle \\ &= -\sum_\rho \left[\tilde{X}^g_{y,\omega_1}\right]_\rho\left[D^f_z\right]_\rho - \sum_\rho\left[\tilde{X}^g_{z,\omega_2}\right]_\rho\left[D^f_y\right]_\rho, \end{aligned} \tag{17}$$

where

$$\left[D^k_z\right]_\rho = \langle\Phi_\rho|\hat{\bar{\mu}}_z R^k|\Phi_0\rangle \tag{18}$$

and

$$\left[\tilde{D}^k_z\right]_\rho = \langle\Phi_0|L^k\hat{\bar{\mu}}_z|\Phi_\rho\rangle \tag{19}$$

are the response intermediates; the programmable expressions for these intermediates are given in the Appendix. The response wave functions are computed by solving the following systems of linear equations:

$$\sum_\nu\left[\hat{\bar{H}} - E^k - \omega\right]_{\rho\nu}\left[X^k_{y,\omega}\right] = \left[D^k_y\right]_\rho \tag{20}$$

and

$$\sum_\rho\left[\tilde{X}^k_{y,\omega}\right]_\rho\left[\hat{\bar{H}} - E^k - \omega\right]_{\rho\nu} = \left[\tilde{D}^k_y\right]_\nu. \tag{21}$$

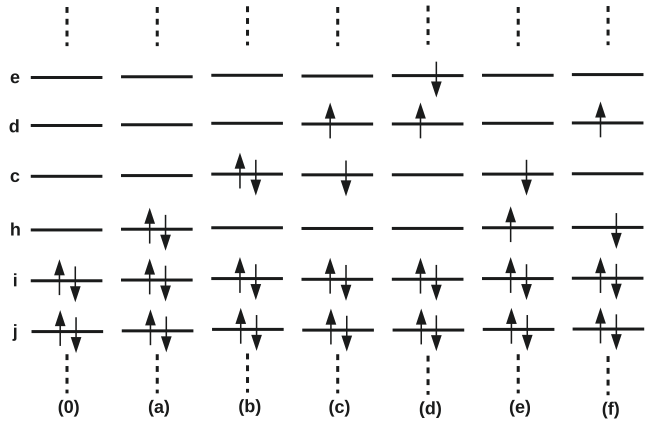

FIG. 1. Target configurations in the EOM-DEA-CCSD method. (0) Dicationic reference. (a) $\Psi^{h\bar{h}}$. (b) $\Psi^{c\bar{c}}$. (c) $\Psi^{d\bar{c}}$. (d) $\Psi^{d\bar{e}}$. (e) $\Psi^{h\bar{c}}$. (f) $\Psi^{d\bar{h}}$. Target states with leading configurations of the type (a)–(f) are well described by the EOM-DEA-CCSD method, as these configurations are all of the type *VV*. Configurations (b)–(f) are also present in the EOM-EE-CCSD method starting with configuration (a) as the reference (Φ_0). Within EOM-EE-CCSD, these configurations are denoted as $\Psi^{c\bar{c}}_{h\bar{h}}$, $\Psi^{d\bar{c}}_{h\bar{h}}$, $\Psi^{d\bar{e}}_{h\bar{h}}$, $\Psi^{c}_{\bar{h}}$, and Ψ^{d}_{h}, respectively. Because the configurations (b)–(d) and (e)–(f) appear at different excitation levels (doubles and singles, respectively), EOM-EE-CCSD does not describe well target states in which configurations of the types (b), (c), and/or (d) have large weights. Triple excitations that appear in higher-level methods (e.g., CC3 and EOM-EE-CCSDT) mitigate this imbalance and enable a more accurate treatment of these target states. Note that this figure does not show the spin complements of configurations (c)–(f), i.e., $\Psi^{c\bar{d}}$, $\Psi^{e\bar{d}}$, $\Psi^{c\bar{h}}$, and $\Psi^{h\bar{d}}$ within EOM-DEA-CCSD for brevity.

III. CONFIGURATIONAL ANALYSIS OF 2PA CHANNELS

Whereas the quality of computed one-photon transition moments depends on how well the wave functions of the initial and final states are described within an approximate *ab initio* framework, the quality of computed 2PA transition moments depends on the full spectrum of the approximate model Hamiltonian, owing to the SOS expressions in Eqs. (10) and (11). This makes the calculations of 2PA cross sections more demanding compared to one-photon transitions. In this section, we carry out a configurational analysis of the EOM-EE and EOM-DEA manifolds in order to better understand the performance of EOM-DEA-CCSD for 2PA cross sections. Toward this goal, we analyze 2PA transition moments in terms of leading configurations. We define a 2PA configurational channel as an SOS term of the 2PA transition moment in which the initial, intermediate, and final wave functions are approximated by their leading electronic configuration (or Slater determinant).[58] We compare the component 2PA configurational channels for EOM-DEA-CCSD, EOM-EE-CCSD, and higher-level methods such as the CC3 response theory or the EOM-EE-CCSDT. In this qualitative analysis, we neglect dynamical correlation and replace $\hat{\bar{\mu}}$ by $\hat{\mu}$ (this is equivalent to setting the T amplitudes to zero) and approximate state energies with orbital energy differences in Eqs. (12) and (13). Such deconstruction of the 2PA SOS terms affords a qualitative assessment of the impact of different configurational manifolds in different excited-state methods such as EOM-DEA-CCSD, EOM-EE-CCSD, EOM-EE-CCSDT, etc. Our aim is to understand which 2PA channels are well or poorly described by different EOM-CC methods, depending on whether the initial, final, or intermediate wave functions are well or poorly described.

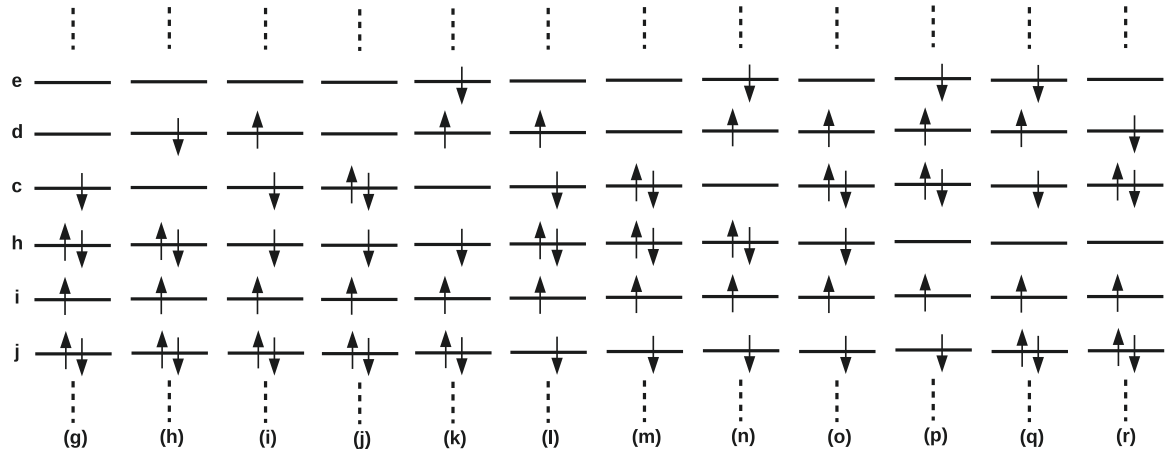

FIG. 2. Target configurations [in addition to configurations (a)–(f)] that can couple to initial configurations (a) and (b) in Fig. 1 via 2PA in an uncorrelated picture. The EOM-DEA-CC notation is given first, and the EOM-EE-CC designation is shown in parentheses. (g) $\Psi^{h\bar{h}\bar{c}}_{i}$ ($\Psi^{\bar{c}}_{i}$). (h) $\Psi^{hh\bar{d}}_{i}$ ($\Psi^{\bar{d}}_{i}$). (i) $\Psi^{d\bar{h}\bar{c}}_{i}$ ($\Psi^{d\bar{c}}_{h\bar{i}}$). (j) $\Psi^{c\bar{h}\bar{c}}_{i}$ ($\Psi^{c\bar{c}}_{h\bar{i}}$). (k) $\Psi^{d\bar{h}\bar{e}}_{i}$ ($\Psi^{d\bar{e}}_{h\bar{i}}$). (l) $\Psi^{hc\bar{h}\bar{c}}_{ji}$ ($\Psi^{c\bar{c}}_{ji}$). (m) $\Psi^{hd\bar{h}\bar{c}}_{ji}$ ($\Psi^{d\bar{c}}_{ji}$). (n) $\Psi^{hd\bar{h}\bar{e}}_{ji}$ ($\Psi^{d\bar{e}}_{ji}$). (o) $\Psi^{cd\bar{h}\bar{c}}_{ji}$ ($\Psi^{cd\bar{c}}_{hji}$). (p) $\Psi^{cd\bar{c}\bar{e}}_{ji}$ ($\Psi^{d\bar{c}}_{hj\bar{h}i}$). (q) $\Psi^{d\bar{c}\bar{e}}_{i}$ ($\Psi^{d\bar{c}\bar{e}}_{h\bar{h}i}$). (r) $\Psi^{c\bar{c}\bar{d}}_{i}$ ($\Psi^{c\bar{c}\bar{d}}_{h\bar{h}i}$). Configurations (l)–(p) are not accessible within the EOM-DEA-CCSD method with configuration (0) as the reference. In contrast, configurations (o)–(r) are not accessible within the EOM-EE-CCSD setup with configuration (a) as the reference. Initial configuration (a) can couple to all final configurations except for configurations (o)–(r). Initial configuration (b) can couple to all final configurations except configurations (h), (k), (l), and (n). Note that this figure does not show the spin complements of these configurations for brevity.

TABLE I. Configurational analysis of the leading channels in the 2PA moment, $M^{g\leftarrow f}$, for the EOM-DEA-CCSD and EOM-EE-CCSD methods. Here, the initial uncorrelated state is approximated by the configuration (a) in Fig. 1 and represented as $\Psi^g \approx \Phi^{h\bar{h}}$ and $\Psi^g \approx \Phi_0$ for the two methods, respectively. Six different configurations [(a), (c), (e), (g), (i), and (l) in Figs. 1 and 2] are considered below as Ψ^f. These channels can couple to Ψ^g via 2PA in the uncorrelated picture through different intermediate states (Ψ^n) approximated by single configurations. The Cartesian indices of $\hat{\mu}$ are omitted for brevity.

	EOM-DEA-CCSD			EOM-EE-CCSD		
Conf. #[1]	Ψ^f	$\frac{\langle\Psi^g\lvert\hat{\mu}\rvert\Psi^n\rangle\langle\Psi^n\lvert\hat{\mu}\rvert\Psi^f\rangle}{E^n-E^g-\omega}$	Comment	Ψ^f	$\frac{\langle\Psi^g\lvert\hat{\mu}\rvert\Psi^n\rangle\langle\Psi^n\lvert\hat{\mu}\rvert\Psi^f\rangle}{E^n-E^g-\omega}$	Comment
(a)	$\Phi^{h\bar{h}}$	$\frac{\langle\Phi^{h\bar{h}}\lvert\hat{\mu}\rvert\Phi^{h\bar{c}}\rangle\langle\Phi^{h\bar{c}}\lvert\hat{\mu}\rvert\Phi^{h\bar{h}}\rangle}{\varepsilon_c-\varepsilon_h-\omega}$	All states well described	Φ_0	$\frac{\langle\Phi_0\lvert\hat{\mu}\rvert\Phi_{\bar{h}}^{\bar{c}}\rangle\langle\Phi_{\bar{h}}^{\bar{c}}\lvert\hat{\mu}\rvert\Phi_0\rangle}{\varepsilon_c-\varepsilon_h-\omega}$	All states well described
		$\frac{\langle\Phi^{h\bar{h}}\lvert\hat{\mu}\rvert\Phi_{\bar{i}}^{h\bar{h}\bar{c}}\rangle\langle\Phi_{\bar{i}}^{h\bar{h}\bar{c}}\lvert\hat{\mu}\rvert\Phi^{h\bar{h}}\rangle}{\varepsilon_c-\varepsilon_i-\omega}$	Intermediate states not well described		$\frac{\langle\Phi_0\lvert\hat{\mu}\rvert\Phi_{\bar{i}}^{\bar{c}}\rangle\langle\Phi_{\bar{i}}^{\bar{c}}\lvert\hat{\mu}\rvert\Phi_0\rangle}{\varepsilon_c-\varepsilon_i-\omega}$	All states well described
(c)	$\Phi^{d\bar{c}}$	$\frac{\langle\Phi^{h\bar{h}}\lvert\hat{\mu}\rvert\Phi^{h\bar{c}}\rangle\langle\Phi^{h\bar{c}}\lvert\hat{\mu}\rvert\Phi^{d\bar{c}}\rangle}{\varepsilon_c-\varepsilon_h-\omega}$	All states well described	$\Phi_{h\bar{h}}^{d\bar{c}}$	$\frac{\langle\Phi_0\lvert\hat{\mu}\rvert\Phi_{\bar{h}}^{\bar{c}}\rangle\langle\Phi_{\bar{h}}^{\bar{c}}\lvert\hat{\mu}\rvert\Phi_{h\bar{h}}^{d\bar{c}}\rangle}{\varepsilon_c-\varepsilon_h-\omega}$	Final state not well described
		$\frac{\langle\Phi^{h\bar{h}}\lvert\hat{\mu}\rvert\Phi^{d\bar{h}}\rangle\langle\Phi^{d\bar{h}}\lvert\hat{\mu}\rvert\Phi^{d\bar{c}}\rangle}{\varepsilon_d-\varepsilon_h-\omega}$	All states well described		$\frac{\langle\Phi_0\lvert\hat{\mu}\rvert\Phi_h^d\rangle\langle\Phi_h^d\lvert\hat{\mu}\rvert\Phi_{h\bar{h}}^{d\bar{c}}\rangle}{\varepsilon_d-\varepsilon_h-\omega}$	Final state not well described
(e)	$\Phi^{h\bar{c}}$	$\frac{\langle\Phi^{h\bar{h}}\lvert\hat{\mu}\rvert\Phi^{h\bar{d}}\rangle\langle\Phi^{h\bar{d}}\lvert\hat{\mu}\rvert\Phi^{h\bar{c}}\rangle}{\varepsilon_d-\varepsilon_h-\omega}$	All states well described	$\Phi_{\bar{h}}^{\bar{c}}$	$\frac{\langle\Phi_0\lvert\hat{\mu}\rvert\Phi_{\bar{h}}^{\bar{d}}\rangle\langle\Phi_{\bar{h}}^{\bar{d}}\lvert\hat{\mu}\rvert\Phi_{\bar{h}}^{\bar{c}}\rangle}{\varepsilon_d-\varepsilon_h-\omega}$	All states well described
		$\frac{\langle\Phi^{h\bar{h}}\lvert\hat{\mu}\rvert\Phi^{h\bar{h}}\rangle\langle\Phi^{h\bar{h}}\lvert\hat{\mu}\rvert\Phi^{h\bar{c}}\rangle}{-\omega}$	All states well described		$\frac{\langle\Phi_0\lvert\hat{\mu}\rvert\Phi_0\rangle\langle\Phi_0\lvert\hat{\mu}\rvert\Phi_{\bar{h}}^{\bar{c}}\rangle}{-\omega}$	All states well described
		$\frac{\langle\Phi^{h\bar{h}}\lvert\hat{\mu}\rvert\Phi_{\bar{i}}^{h\bar{h}\bar{c}}\rangle\langle\Phi_{\bar{i}}^{h\bar{h}\bar{c}}\lvert\hat{\mu}\rvert\Phi^{h\bar{c}}\rangle}{\varepsilon_c-\varepsilon_i-\omega}$	Intermediate states not well described		$\frac{\langle\Phi_0\lvert\hat{\mu}\rvert\Phi_{\bar{i}}^{\bar{c}}\rangle\langle\Phi_{\bar{i}}^{\bar{c}}\lvert\hat{\mu}\rvert\Phi_{\bar{h}}^{\bar{c}}\rangle}{\varepsilon_c-\varepsilon_i-\omega}$	All states well described
(g)	$\Phi_{\bar{i}}^{h\bar{h}\bar{c}}$	$\frac{\langle\Phi^{h\bar{h}}\lvert\hat{\mu}\rvert\Phi_{\bar{i}}^{h\bar{h}\bar{d}}\rangle\langle\Phi_{\bar{i}}^{h\bar{h}\bar{d}}\lvert\hat{\mu}\rvert\Phi_{\bar{i}}^{h\bar{h}\bar{c}}\rangle}{\varepsilon_d-\varepsilon_i-\omega}$	Final and intermediate states not well described	$\Phi_{\bar{i}}^{\bar{c}}$	$\frac{\langle\Phi_0\lvert\hat{\mu}\rvert\Phi_{\bar{i}}^{\bar{d}}\rangle\langle\Phi_{\bar{i}}^{\bar{d}}\lvert\hat{\mu}\rvert\Phi_{\bar{i}}^{\bar{c}}\rangle}{\varepsilon_d-\varepsilon_i-\omega}$	All states well described
		$\frac{\langle\Phi^{h\bar{h}}\lvert\hat{\mu}\rvert\Phi^{h\bar{h}}\rangle\langle\Phi^{h\bar{h}}\lvert\hat{\mu}\rvert\Phi_{\bar{i}}^{h\bar{h}\bar{c}}\rangle}{-\omega}$	Final state not well described		$\frac{\langle\Phi_0\lvert\hat{\mu}\rvert\Phi_0\rangle\langle\Phi_0\lvert\hat{\mu}\rvert\Phi_{\bar{i}}^{\bar{c}}\rangle}{-\omega}$	All states well described
		$\frac{\langle\Phi^{h\bar{h}}\lvert\hat{\mu}\rvert\Phi^{h\bar{c}}\rangle\langle\Phi^{h\bar{c}}\lvert\hat{\mu}\rvert\Phi_{\bar{i}}^{h\bar{h}\bar{c}}\rangle}{\varepsilon_c-\varepsilon_h-\omega}$	Final state not well described		$\frac{\langle\Phi_0\lvert\hat{\mu}\rvert\Phi_{\bar{h}}^{\bar{c}}\rangle\langle\Phi_{\bar{h}}^{\bar{c}}\lvert\hat{\mu}\rvert\Phi_{\bar{i}}^{\bar{c}}\rangle}{\varepsilon_c-\varepsilon_h-\omega}$	All states well described
		$\frac{\langle\Phi^{h\bar{h}}\lvert\hat{\mu}\rvert\Phi_{\bar{j}}^{h\bar{h}\bar{c}}\rangle\langle\Phi_{\bar{j}}^{h\bar{h}\bar{c}}\lvert\hat{\mu}\rvert\Phi_{\bar{i}}^{h\bar{h}\bar{c}}\rangle}{\varepsilon_c-\varepsilon_j-\omega}$	Final and intermediate states not well described		$\frac{\langle\Phi_0\lvert\hat{\mu}\rvert\Phi_{\bar{j}}^{\bar{c}}\rangle\langle\Phi_{\bar{j}}^{\bar{c}}\lvert\hat{\mu}\rvert\Phi_{\bar{i}}^{\bar{c}}\rangle}{\varepsilon_c-\varepsilon_j-\omega}$	All states well described
(i)	$\Phi_{\bar{i}}^{d\bar{h}\bar{c}}$	$\frac{\langle\Phi^{h\bar{h}}\lvert\hat{\mu}\rvert\Phi_{\bar{i}}^{h\bar{h}\bar{c}}\rangle\langle\Phi_{\bar{i}}^{h\bar{h}\bar{c}}\lvert\hat{\mu}\rvert\Phi_{\bar{i}}^{d\bar{h}\bar{c}}\rangle}{\varepsilon_c-\varepsilon_i-\omega}$	Final and intermediate states not well described	$\Phi_{h\bar{i}}^{d\bar{c}}$	$\frac{\langle\Phi_0\lvert\hat{\mu}\rvert\Phi_{\bar{i}}^{\bar{c}}\rangle\langle\Phi_{\bar{i}}^{\bar{c}}\lvert\hat{\mu}\rvert\Phi_{h\bar{i}}^{d\bar{c}}\rangle}{\varepsilon_c-\varepsilon_i-\omega}$	Final state not well described
		$\frac{\langle\Phi^{h\bar{h}}\lvert\hat{\mu}\rvert\Phi^{d\bar{h}}\rangle\langle\Phi^{d\bar{h}}\lvert\hat{\mu}\rvert\Phi_{\bar{i}}^{d\bar{h}\bar{c}}\rangle}{\varepsilon_d-\varepsilon_h-\omega}$	Final state not well described		$\frac{\langle\Phi_0\lvert\hat{\mu}\rvert\Phi_h^d\rangle\langle\Phi_h^d\lvert\hat{\mu}\rvert\Phi_{h\bar{i}}^{d\bar{c}}\rangle}{\varepsilon_d-\varepsilon_h-\omega}$	Final state not well described
(l)	$\Phi_{j\bar{i}}^{hd\bar{h}\bar{c}}$	-	Final configuration absent	$\Phi_{j\bar{i}}^{d\bar{c}}$	$\frac{\langle\Phi_0\lvert\hat{\mu}\rvert\Phi_{\bar{i}}^{\bar{c}}\rangle\langle\Phi_{\bar{i}}^{\bar{c}}\lvert\hat{\mu}\rvert\Phi_{j\bar{i}}^{d\bar{c}}\rangle}{\varepsilon_c-\varepsilon_i-\omega}$	Final state not well described
		-	Final configuration absent		$\frac{\langle\Phi_0\lvert\hat{\mu}\rvert\Phi_j^d\rangle\langle\Phi_j^d\lvert\hat{\mu}\rvert\Phi_{j\bar{i}}^{d\bar{c}}\rangle}{\varepsilon_d-\varepsilon_j-\omega}$	Final state not well described

[1]Relative to the initial configuration, individual configurations within the sets [(b), (c), (d)], [(e), (f)], [(g), (h)], [(i), (j), (k)] and [(l), (m), (n)] are similar. The table, therefore, presents the 2PA channels involving just one configuration from these sets of final configurations.

TABLE II. Configurational analysis of the leading channels in the 2PA moment, $M^{g\leftarrow f}$, for the EOM-DEA-CCSD and EOM-EE-CCSD methods. Here, the initial uncorrelated state is approximated by configuration (b) in Fig. 1 and represented as $\Psi^g \approx \Phi^{c\bar{c}}$ and $\Psi^g \approx \Phi^{c\bar{c}}_{h\bar{h}}$ for the two methods, respectively. Six different configurations are considered below as Ψ^f, as described by configurations (a)–(f) in Fig. 1. These channels can couple to Ψ^g via 2PA in the uncorrelated picture through different intermediate states (Ψ^n) approximated by single configurations. The Cartesian indices of $\hat{\mu}$ are omitted for brevity.

	EOM-DEA-CCSD			EOM-EE-CCSD		
Conf. #	Ψ^f	$\frac{\langle\Psi^g\lvert\hat{\mu}\rvert\Psi^n\rangle\langle\Psi^n\lvert\hat{\mu}\rvert\Psi^f\rangle}{E^n-E^g-\omega}$	Comment	Ψ^f	$\frac{\langle\Psi^g\lvert\hat{\mu}\rvert\Psi^n\rangle\langle\Psi^n\lvert\hat{\mu}\rvert\Psi^f\rangle}{E^n-E^g-\omega}$	Comment
(a)	$\Phi^{h\bar{h}}$	$\frac{\langle\Phi^{c\bar{c}}\lvert\hat{\mu}\rvert\Phi^{h\bar{c}}\rangle\langle\Phi^{h\bar{c}}\lvert\hat{\mu}\rvert\Phi^{h\bar{h}}\rangle}{\varepsilon_h-\varepsilon_c-\omega}$	All states well described	Φ_0	$\frac{\langle\Phi^{c\bar{c}}_{h\bar{h}}\lvert\hat{\mu}\rvert\Phi^{\bar{c}}_{\bar{h}}\rangle\langle\Phi^{\bar{c}}_{\bar{h}}\lvert\hat{\mu}\rvert\Phi_0\rangle}{\varepsilon_h-\varepsilon_c-\omega}$	Initial state not well described
(b)	$\Phi^{c\bar{c}}$	$\frac{\langle\Phi^{c\bar{c}}\lvert\hat{\mu}\rvert\Phi^{c\bar{c}}\rangle\langle\Phi^{c\bar{c}}\lvert\hat{\mu}\rvert\Phi^{c\bar{c}}\rangle}{-\omega}$	All states well described	$\Phi^{c\bar{c}}_{h\bar{h}}$	$\frac{\langle\Phi^{c\bar{c}}_{h\bar{h}}\lvert\hat{\mu}\rvert\Phi^{c\bar{c}}_{h\bar{h}}\rangle\langle\Phi^{c\bar{c}}_{h\bar{h}}\lvert\hat{\mu}\rvert\Phi^{c\bar{c}}_{h\bar{h}}\rangle}{-\omega}$	No state well described
		$\frac{\langle\Phi^{c\bar{c}}\lvert\hat{\mu}\rvert\Phi^{c\bar{c}\bar{e}}_{i}\rangle\langle\Phi^{c\bar{c}\bar{e}}_{i}\lvert\hat{\mu}\rvert\Phi^{c\bar{c}}\rangle}{\varepsilon_e-\varepsilon_i-\omega}$	Intermediate states not well described		$\frac{\langle\Phi^{c\bar{c}}_{h\bar{h}}\lvert\hat{\mu}\rvert\Phi^{c\bar{c}\bar{e}}_{h\bar{h}i}\rangle\langle\Phi^{c\bar{c}\bar{e}}_{h\bar{h}i}\lvert\hat{\mu}\rvert\Phi^{c\bar{c}}_{h\bar{h}}\rangle}{\varepsilon_e-\varepsilon_i-\omega}$	Initial and final states not well described; intermediate states absent
		$\frac{\langle\Phi^{c\bar{c}}\lvert\hat{\mu}\rvert\Phi^{h\bar{c}}\rangle\langle\Phi^{h\bar{c}}\lvert\hat{\mu}\rvert\Phi^{c\bar{c}}\rangle}{\varepsilon_h-\varepsilon_c-\omega}$	All states well described		$\frac{\langle\Phi^{c\bar{c}}_{h\bar{h}}\lvert\hat{\mu}\rvert\Phi^{\bar{c}}_{\bar{h}}\rangle\langle\Phi^{\bar{c}}_{\bar{h}}\lvert\hat{\mu}\rvert\Phi^{c\bar{c}}_{h\bar{h}}\rangle}{\varepsilon_h-\varepsilon_c-\omega}$	Initial and final states not well described
		$\frac{\langle\Phi^{c\bar{c}}\lvert\hat{\mu}\rvert\Phi^{hc\bar{c}}_{i}\rangle\langle\Phi^{hc\bar{c}}_{i}\lvert\hat{\mu}\rvert\Phi^{c\bar{c}}\rangle}{\varepsilon_h-\varepsilon_i-\omega}$	Intermediate states not well described		$\frac{\langle\Phi^{c\bar{c}}_{h\bar{h}}\lvert\hat{\mu}\rvert\Phi^{c\bar{c}}_{i\bar{h}}\rangle\langle\Phi^{c\bar{c}}_{i\bar{h}}\lvert\hat{\mu}\rvert\Phi^{c\bar{c}}_{h\bar{h}}\rangle}{\varepsilon_h-\varepsilon_i-\omega}$	No state well described
		$\frac{\langle\Phi^{c\bar{c}}\lvert\hat{\mu}\rvert\Phi^{d\bar{c}}\rangle\langle\Phi^{d\bar{c}}\lvert\hat{\mu}\rvert\Phi^{c\bar{c}}\rangle}{\varepsilon_d-\varepsilon_c-\omega}$	All states well described		$\frac{\langle\Phi^{c\bar{c}}_{h\bar{h}}\lvert\hat{\mu}\rvert\Phi^{d\bar{c}}_{h\bar{h}}\rangle\langle\Phi^{d\bar{c}}_{h\bar{h}}\lvert\hat{\mu}\rvert\Phi^{c\bar{c}}_{h\bar{h}}\rangle}{\varepsilon_d-\varepsilon_c-\omega}$	No state well described
(c)	$\Phi^{d\bar{c}}$	$\frac{\langle\Phi^{c\bar{c}}\lvert\hat{\mu}\rvert\Phi^{c\bar{c}}\rangle\langle\Phi^{c\bar{c}}\lvert\hat{\mu}\rvert\Phi^{d\bar{c}}\rangle}{-\omega}$	All states well described	$\Phi^{c\bar{c}}_{h\bar{h}}$	$\frac{\langle\Phi^{c\bar{c}}_{h\bar{h}}\lvert\hat{\mu}\rvert\Phi^{c\bar{c}}_{h\bar{h}}\rangle\langle\Phi^{c\bar{c}}_{h\bar{h}}\lvert\hat{\mu}\rvert\Phi^{d\bar{c}}_{h\bar{h}}\rangle}{-\omega}$	No state well described
		$\frac{\langle\Phi^{c\bar{c}}\lvert\hat{\mu}\rvert\Phi^{dc\bar{c}}_{i}\rangle\langle\Phi^{dc\bar{c}}_{i}\lvert\hat{\mu}\rvert\Phi^{d\bar{c}}\rangle}{\varepsilon_d-\varepsilon_i-\omega}$	Intermediate states not well described		$\frac{\langle\Phi^{c\bar{c}}_{h\bar{h}}\lvert\hat{\mu}\rvert\Phi^{dc\bar{c}}_{ih\bar{h}}\rangle\langle\Phi^{dc\bar{c}}_{ih\bar{h}}\lvert\hat{\mu}\rvert\Phi^{d\bar{c}}_{h\bar{h}}\rangle}{\varepsilon_d-\varepsilon_i-\omega}$	Initial and final states not well described; intermediate states absent
		$\frac{\langle\Phi^{c\bar{c}}\lvert\hat{\mu}\rvert\Phi^{h\bar{c}}\rangle\langle\Phi^{h\bar{c}}\lvert\hat{\mu}\rvert\Phi^{d\bar{c}}\rangle}{\varepsilon_h-\varepsilon_c-\omega}$	All states well described		$\frac{\langle\Phi^{c\bar{c}}_{h\bar{h}}\lvert\hat{\mu}\rvert\Phi^{\bar{c}}_{\bar{h}}\rangle\langle\Phi^{\bar{c}}_{\bar{h}}\lvert\hat{\mu}\rvert\Phi^{d\bar{c}}_{h\bar{h}}\rangle}{\varepsilon_h-\varepsilon_c-\omega}$	Initial and final states not well described
		$\frac{\langle\Phi^{c\bar{c}}\lvert\hat{\mu}\rvert\Phi^{d\bar{c}}\rangle\langle\Phi^{d\bar{c}}\lvert\hat{\mu}\rvert\Phi^{d\bar{c}}\rangle}{\varepsilon_d-\varepsilon_c-\omega}$	All states well described		$\frac{\langle\Phi^{c\bar{c}}_{h\bar{h}}\lvert\hat{\mu}\rvert\Phi^{d\bar{c}}_{h\bar{h}}\rangle\langle\Phi^{d\bar{c}}_{h\bar{h}}\lvert\hat{\mu}\rvert\Phi^{d\bar{c}}_{h\bar{h}}\rangle}{\varepsilon_d-\varepsilon_c-\omega}$	No state well described
(d)	$\Phi^{d\bar{e}}$	$\frac{\langle\Phi^{c\bar{c}}\lvert\hat{\mu}\rvert\Phi^{c\bar{e}}\rangle\langle\Phi^{c\bar{e}}\lvert\hat{\mu}\rvert\Phi^{d\bar{e}}\rangle}{\varepsilon_e-\varepsilon_c-\omega}$	All states well described	$\Phi^{d\bar{e}}_{h\bar{h}}$	$\frac{\langle\Phi^{c\bar{c}}_{h\bar{h}}\lvert\hat{\mu}\rvert\Phi^{c\bar{e}}_{h\bar{h}}\rangle\langle\Phi^{c\bar{e}}_{h\bar{h}}\lvert\hat{\mu}\rvert\Phi^{d\bar{e}}_{h\bar{h}}\rangle}{\varepsilon_e-\varepsilon_c-\omega}$	No state well described
(e)	$\Phi^{h\bar{c}}$	$\frac{\langle\Phi^{c\bar{c}}\lvert\hat{\mu}\rvert\Phi^{c\bar{c}}\rangle\langle\Phi^{c\bar{c}}\lvert\hat{\mu}\rvert\Phi^{h\bar{c}}\rangle}{-\omega}$	All states well described	$\Phi^{\bar{c}}_{\bar{h}}$	$\frac{\langle\Phi^{c\bar{c}}_{h\bar{h}}\lvert\hat{\mu}\rvert\Phi^{c\bar{c}}_{h\bar{h}}\rangle\langle\Phi^{c\bar{c}}_{h\bar{h}}\lvert\hat{\mu}\rvert\Phi^{\bar{c}}_{\bar{h}}\rangle}{-\omega}$	Only the final state well described
		$\frac{\langle\Phi^{c\bar{c}}\lvert\hat{\mu}\rvert\Phi^{h\bar{c}}\rangle\langle\Phi^{h\bar{c}}\lvert\hat{\mu}\rvert\Phi^{h\bar{c}}\rangle}{\varepsilon_h-\varepsilon_c-\omega}$	All states well described		$\frac{\langle\Phi^{c\bar{c}}_{h\bar{h}}\lvert\hat{\mu}\rvert\Phi^{\bar{c}}_{\bar{h}}\rangle\langle\Phi^{\bar{c}}_{\bar{h}}\lvert\hat{\mu}\rvert\Phi^{\bar{c}}_{\bar{h}}\rangle}{\varepsilon_h-\varepsilon_c-\omega}$	Initial state not well described
		$\frac{\langle\Phi^{c\bar{c}}\lvert\hat{\mu}\rvert\Phi^{d\bar{c}}\rangle\langle\Phi^{d\bar{c}}\lvert\hat{\mu}\rvert\Phi^{h\bar{c}}\rangle}{\varepsilon_d-\varepsilon_c-\omega}$	All states well described		$\frac{\langle\Phi^{c\bar{c}}_{h\bar{h}}\lvert\hat{\mu}\rvert\Phi^{d\bar{c}}_{h\bar{h}}\rangle\langle\Phi^{d\bar{c}}_{h\bar{h}}\lvert\hat{\mu}\rvert\Phi^{\bar{c}}_{\bar{h}}\rangle}{\varepsilon_d-\varepsilon_c-\omega}$	Only the final state well described
		$\frac{\langle\Phi^{c\bar{c}}\lvert\hat{\mu}\rvert\Phi^{hc\bar{c}}_{i}\rangle\langle\Phi^{hc\bar{c}}_{i}\lvert\hat{\mu}\rvert\Phi^{h\bar{c}}\rangle}{\varepsilon_h-\varepsilon_i-\omega}$	Intermediate states not well described		$\frac{\langle\Phi^{c\bar{c}}_{h\bar{h}}\lvert\hat{\mu}\rvert\Phi^{c\bar{c}}_{i\bar{h}}\rangle\langle\Phi^{c\bar{c}}_{i\bar{h}}\lvert\hat{\mu}\rvert\Phi^{\bar{c}}_{\bar{h}}\rangle}{\varepsilon_h-\varepsilon_i-\omega}$	Only the final state well described
(f)	$\Phi^{d\bar{h}}$	$\frac{\langle\Phi^{c\bar{c}}\lvert\hat{\mu}\rvert\Phi^{d\bar{c}}\rangle\langle\Phi^{d\bar{c}}\lvert\hat{\mu}\rvert\Phi^{d\bar{h}}\rangle}{\varepsilon_d-\varepsilon_c-\omega}$	All states well described	Φ^{d}_{h}	$\frac{\langle\Phi^{c\bar{c}}_{h\bar{h}}\lvert\hat{\mu}\rvert\Phi^{d\bar{c}}_{h\bar{h}}\rangle\langle\Phi^{d\bar{c}}_{h\bar{h}}\lvert\hat{\mu}\rvert\Phi^{d}_{h}\rangle}{\varepsilon_d-\varepsilon_c-\omega}$	Only the final state well described
		$\frac{\langle\Phi^{c\bar{c}}\lvert\hat{\mu}\rvert\Phi^{c\bar{h}}\rangle\langle\Phi^{c\bar{h}}\lvert\hat{\mu}\rvert\Phi^{d\bar{h}}\rangle}{\varepsilon_h-\varepsilon_c-\omega}$	All states well described		$\frac{\langle\Phi^{c\bar{c}}_{h\bar{h}}\lvert\hat{\mu}\rvert\Phi^{c}_{h}\rangle\langle\Phi^{c}_{h}\lvert\hat{\mu}\rvert\Phi^{d}_{h}\rangle}{\varepsilon_h-\varepsilon_c-\omega}$	Only the final state well described

In this section, labels i, j, ... refer to occupied orbitals other than the HOMO; labels d, e, ... refer to unoccupied orbitals other than the lowest unoccupied MO (LUMO); label h refers to the HOMO; label c refers to the LUMO; and labels p and $\bar{p}$ refer to alpha and beta spin orbital p with energy ε_p, respectively.

In general, wave functions for which the leading configurations are of the type VV, as represented by the target configurations in Fig. 1, are well described by the EOM-DEA-CCSD method. This is the case for ground-state wave functions in the test systems we consider in this study, which are dominated by configurations (a) and (b). In what follows, we will set our initial wave function in the 2PA channels as one of these two target configurations one at a time, identify the final configurations that can couple to the chosen initial configuration via 2PA, and then assess the constructed 2PA channels.

Figure 2 illustrates the exemplary final configurations that can couple with configurations (a) and (b) in Fig. 1 within the uncorrelated setup of 2PA channels. Tables I and II give the various 2PA channels that can be constructed between these initial and final configurations via intermediate configurations for both the EOM-EE-CCSD and EOM-DEA-CCSD methods. Since the EOM-EE-CCSD method can only well describe target states that do not have significant doubly excited character, only the 2PA channels with initial configuration (a) and final singly excited configurations (a), (e), (f), (g), and (h) are well described {note that in Table I, we do not consider final configurations (f) and (h) as relative to the initial conformation (a), configurations in sets [(e), (f)] and [(g), (h)] are similar}. The intermediate configurations in these 2PA channels are also well described; this is why EOM-EE-CCSD typically performs well for ground-to-singly-excited 2PA transitions in closed-shell systems. However, for describing transitions between states with significant doubly excited character, EOM-EE-CCSD suffers from inadequate dynamical correlation, and these different transition characters are treated in an unbalanced fashion.[39] The addition of triples in EOM-EE-CCSDT and CC3 response theory mitigates this for a robust treatment of the 2PA transition.

In contrast, EOM-DEA-CCSD performs well for target states for which the wave functions have leading configurations that are singly and/or doubly excited from the HOMO. Consequently, only the 2PA channels with final configurations (a)–(f) in Table I are expected to be well described; 2PA channels involving target states with leading final configurations that involve excitations from orbitals lower than the HOMO are poorly described with EOM-DEA-CCSD. Further, the intermediate configurations for the last sets of 2PA channels involving configurations (e) and (f) are of the type $OVVV$ with excitations involving occupied orbitals other than the HOMO; therefore, these channels are not well described by EOM-DEA-CCSD, despite a balanced treatment of the corresponding initial and final wave functions. We will illustrate this dependency on the intermediate states with our benchmark results.

The second important configuration, configuration (b) in Fig. 1, in the initial wave functions of our test systems can couple to all final configurations in Figs. 1 and 2 except configurations (h), (k), (l), and (n). In Table II, we only consider its coupling to final configurations (a)–(f) in the 2PA channels, as these configurations are well-described with EOM-DEA-CCSD. As Table II shows, these 2PA channels for EOM-DEA-CCSD are relatively well described compared to EOM-EE-CCSD, even though intermediate configurations in a few channels involve excitations from occupied orbitals lower than the HOMO. This is expected as the EOM-EE-CCSD cannot treat target states with dominant doubly excited configurations on an equal footing as the singly excited configurations. However, as we will illustrate below, the EOM-DEA-CCSD treatment of the 2PA moments deteriorates significantly when the final excited-state wave functions have significant contributions from determinants involving excitations from occupied orbitals other than the HOMO.

Note that wave functions dominated by configurations (a)–(n) can be described well with methods involving triples excitations, such as the EOM-EE-CCSDT and the CC3 response theory. However, even these methods cannot describe well the excited-state wave functions dominated by configurations (o)–(r); configurations (o), (q), and (r) are triply excited relative to the reference configuration (a) and configuration (p) is accessible only when quadruple excited determinants are included in the method. However, such states are typically high-lying, and their contribution to the 2PA moments of low-lying transitions is expected to be small due to the larger denominators arising from the larger differences in the excitation energies and the photon energies.

IV. COMPUTATIONAL DETAILS

We implemented the calculation of EOM-DEA-CCSD 2PA cross sections (formulated within the expectation-value approach) in the Q-Chem quantum chemistry package.[59] The EOM-EE-CCSD results were obtained using the previously reported implementation for 2PA cross sections in Q-Chem.[49,60,61] The CC3 response theory results were obtained with the Dalton 2020 package.[62,63]

Our test systems included ethene, twisted ethene, *trans*-butadiene, and all *trans* hexatriene and octatetraene. Hereby, we drop the prefix *trans* for brevity. The geometries of ethene and butadiene are the same as in Ref. 39. For ethene at various HCCH torsion angles, the bond lengths and angles were kept fixed to the respective values for untwisted ethene. We used geometries optimized with RI-MP2/cc-pVQZ and RI-MP2/cc-pVTZ for hexatriene and octatetraene, respectively. All geometries are given in the supplementary material.

We used the dicationic Hartree–Fock reference in all EOM-DEA-CCSD calculations.

We report the results following the Q-Chem symmetry notation rather than the Mulliken symmetry notation—details can be found in Refs. 54, 64, and 65. We used the following Abelian point groups in our calculations: D_{2h} for ethene; D_2 for twisted ethene systems; and C_{2h} for butadiene, hexatriene, and octatetraene.

For twisted ethene, we used Dunning's double zeta basis set (aug-cc-pVDZ). For other systems, we computed excited states and 2PA cross sections with the cc-pVDZ, aug-cc-pVDZ, and aug-cc-pVTZ basis sets. Core orbitals were kept frozen in all EOM-CCSD calculations.

V. RESULTS AND DISCUSSION

A. Twisted ethene

The states of interest in ethene have the following characters: $N\left({}^1(\pi)^2\right)$ (ground state), $V\left({}^1(\pi)^1(\pi^*)^1\right)$, and $Z\left({}^1(\pi^*)^2\right)$.[66] In

TABLE III. Vertical excitation energies (Ω^{fg}) and 2PA cross sections (δ^{fg}) for the N → Z transition in ethene for different HCCH torsion angles (θ) computed with the CC3 quadratic response theory, EOM-DEA-CCSD expectation-value, and EOM-EE-CCSD expectation-value approaches with the aug-cc-pVDZ basis set.

	CC3		EOM-DEA-CCSD		EOM-EE-CCSD	
θ	Ω^{f} (eV)	δ^{fg} (a.u.)	Ω^{fg} (eV)	δ^{fg} (a.u.)	Ω^{fg} (eV)	δ^{fg} (a.u.)
60°	6.28	448.4	5.91	522.1	7.80	1539.9
70°	4.77	245.1	4.41	282.0	6.51	346.5
80°	3.30	118.3	3.11	122.3	4.80	1760.1
90°	2.32	0.4	2.52	0.1	3.34	636.8

addition, the V state includes significant Rydberg contributions. The Z state has a doubly excited character. At the ground-state geometry, it is located high in energy, above the ionization onset (i.e., it is a resonance, embedded in the ionization continuum). However, its energy drops as the HCCH torsion angle is increased from 0° to 90°, as was explained in Ref. 39. At perfectly twisted geometries (90°), the π and π^* orbitals are degenerate, and the potential energy curves for the V and Z states have minima. The orbital degeneracy also leads to the multiconfigurational character of the N state, which increases as the torsion angle is increased from 0° to 90°. This underlying multiconfigurational electronic structure makes these twisted structures a challenging case for a single-reference method such as EOM-EE-CCSD. Reference 39 discusses how the EOM-DEA-CCSD approach reliably describes the torsion barrier and vertical excitation energies in ethene at planar and twisted geometries. Here, we focus on the performance of the EOM-DEA-CCSD for the N → Z 2PA transition in these twisted ethene structures.

Figure 3 compares the energies relative to the ground-state energy (at planar geometry) for the N and Z states and the energies of the N → Z excitation as a function of ethene's torsion angle for the EOM-DEA-CCSD, EOM-EE-CCSD, and CC3 methods with the aug-cc-pVDZ basis set. As expected, EOM-EE-CCSD performs poorly for the Z state even at the perfectly twisted geometry; the N → Z excitation energy is significantly overestimated (raw data in Table III). In contrast, as the torsion angle increases, the doubly excited character of the Z state increases, which is reliably captured by EOM-DEA-CCSD, and the discrepancy between the EOM-DEA-CCSD and CC3 state energies is reduced. In fact, the excitation-energy curves for EOM-DEA-CCSD and CC3 cross between 80° and 90°. Nevertheless, these differences (≈0.2 eV) relative to CC3 energies nearer to the perfectly twisted geometry are smaller, indicating that EOM-DEA-CCSD gives similar quality excitation energies when the multiconfigurational character of the wave function is large. On the other hand, the larger differences between EOM-DEA-CCSD and CC3 energies at smaller torsion angles are a consequence of the inability of the EOM-DEA-CCSD method to treat singly excited configurations from occupied orbitals lower than the HOMO on an equal footing relative to excited configurations from the HOMO; the former configurations have a non-negligible contribution to the CC3 Z-state wave function at smaller torsion angles.

The bottom panel of Fig. 3 compares the cross sections for the N → Z 2PA transition as a function of the torsion angle with the

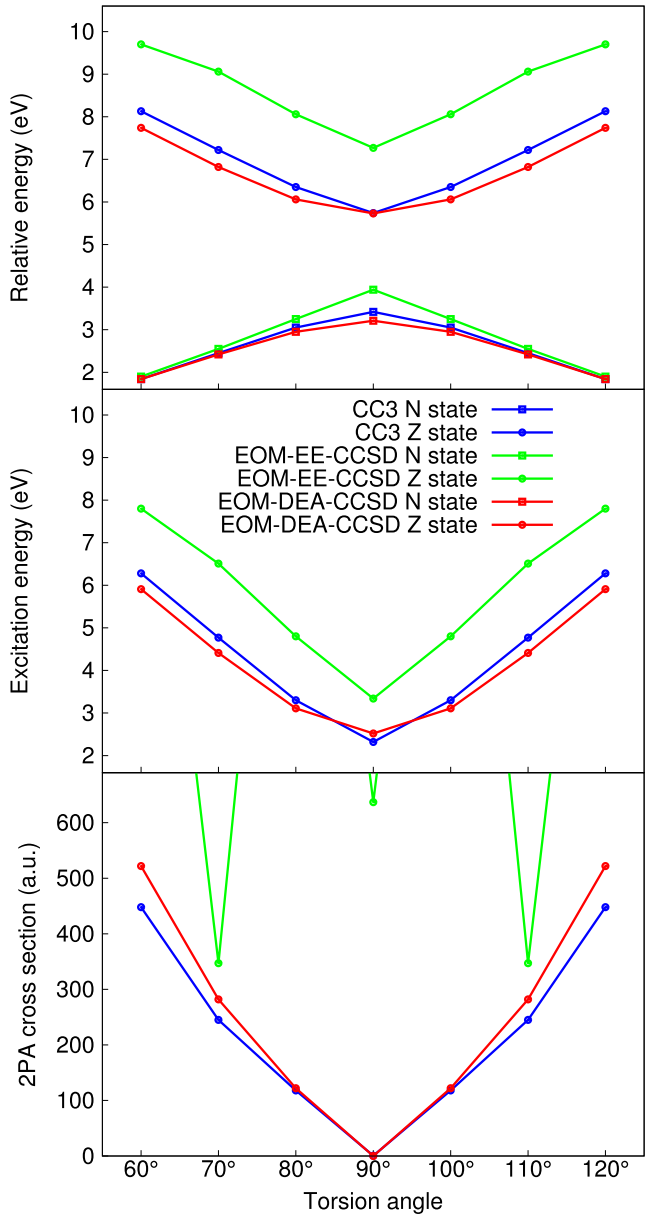

FIG. 3. (Top) State energies of states N and Z relative to the ground state of untwisted ethene, (middle) excitation energies for state Z relative to state N, and (bottom) 2PA cross sections for the N → Z transition in twisted ethene as a function of the HCCH torsion angle computed at the EOM-DEA-CCSD, EOM-EE-CCSD, and CC3 levels of theory and the aug-cc-pVDZ basis set.

EOM-DEA-CCSD, EOM-EE-CCSD, and CC3 levels of theory. The 2PA cross sections decrease as a function of the torsion angle for the EOM-DEA-CCSD and CC3 approaches. This can be explained using the three-state model involving the N, Z, and dominant intermediate V states to explain the decreasing dominant M_{xx}^{NZ} 2PA moments with the torsion angle. The dipole coupling between the N and V states decreases with increasing torsion angle

and becomes negligible for the perfectly twisted ethene, a consequence of the increasing doubly excited character of the N state, as explained in the Appendix. As a result, the dominant SOS term for the M_{xx}^{NZ} moments decreases to zero with increasing torsion angle.

Figure 3 illustrates the much poorer description with EOM-EE-CCSD, as was explained in Sec. III, for the 2PA cross sections involving states with significant double excited character. For twisted ethene, the EOM-EE-CCSD 2PA cross sections rapidly oscillate as the torsion angle is increased between 60° and 90°, in contrast to the monotonously decreasing 2PA cross sections with the EOM-DEA-CCSD and CC3 approaches. This is attributed to the poorly described character of the Z state, with imbalanced contributions of singly and doubly excited configurations, for different torsion angles with the EOM-EE-CCSD method, leading to poor quality transition properties. This is also highlighted by the fact that EOM-EE-CCSD computes non-degenerate Z and V states for the perfectly twisted ethene.

Similar to the trend observed for excitation energies, the 2PA cross sections for this transition show smaller differences between the EOM-DEA-CCSD and CC3 results as the torsion angle is increased up to 90°. The larger differences at lower torsion angles arise, primarily, due to two factors. First, we use the expectation-value approach for computing 2PA moments within the EOM-DEA-CCSD framework as against the CC3 (full) response theory, leading to small differences.[49,51,67] Second, EOM-DEA-CCSD is a lower-level method compared to CC3; the former cannot describe the dynamical correlation as well as the latter. This results in a relatively poorer description of the non-negligible valence and Rydberg characters of the EOM-DEA-CCSD target states at smaller torsion angles compared to that with CC3. On the other hand, as the torsion angle is increased to 90°, the wave function of the N and Z states becomes predominantly multiconfigurational in character [i.e., configurations (a) and (b) in Fig. 1 dominate], which EOM-DEA-CCSD can describe as well as CC3, resulting in smaller differences between the CC3 and EOM-DEA-CCSD results. The reliable description of the electronic structure with EOM-DEA-CCSD is also apparent from the configurational analysis in Tables I and II, which suggests that the 2PA channels are all well described by EOM-DEA-CCSD when the final state has a dominant doubly excited configuration. When the target EOM-DEA-CCSD state has significant contributions from other valence configurations, i.e., at smaller torsion angles, not all the intermediate configurations (and 2PA channels) are well described.

B. Polyenes

Prototypical polyenes such as butadiene, hexatriene, and octatetraene feature close-lying excited states with multiconfigurational (mixed Rydberg and doubly excited) wave functions.[14–17] These systems, therefore, represent challenging cases that give a measure of the balance of dynamical and static correlation captured by a multireference method in the description of these excited-state energies and wave functions. For example, the $2A_g$ (one-photon dark) and $1B_u$ (one-photon bright) singlet states in butadiene and hexatriene have been the focus of many studies, with an evident lack of quantitative agreement among different theoretical methods and experiments with respect to their state ordering. As discussed in Ref. 39, multireference methods typically overestimate the doubly excited contributions in the wave functions for the $2A_g$ state, whereas single-reference methods such as ADC and EOM-EE-CCSD underestimate these contributions. For butadiene, the current consensus is that $1B_u$ is lower than $2A_g$, based on the observed fluorescence in butadiene. Even though this ordering is expected to change for longer polyenes, for hexatriene and octatetraene considered in the present study, EOM-DEA-CCSD places the one-photon dark state above the one-photon bright state, as shown in Table IV.

We consider 2PA transitions with degenerate photons to the two-photon bright $2A_g$ states for these polyenes. In addition, we also consider the N → Z transition ($XA_g \rightarrow 6A_g$ with CC3) in ethene that has a significant doubly excited character (note that the Z state is not accessible with EOM-EE-CCSD[39]). We compare excitation energies and 2PA cross sections computed with the EOM-DEA-CCSD and higher-level CC3 response theory approaches. Table V presents the raw data for the 2PA transitions, which suggests that 2PA cross sections are strongly sensitive to the basis set, as is well documented. For example, the 2PA cross sections for ethene change by almost 50% between the aug-cc-pVDZ and aug-cc-pVTZ basis sets; the change for butadiene and hexatriene is even larger between the cc-pVDZ and aug-cc-pVDZ basis sets. The excitation energies of the $2A_g$ state also follow a similar trend with respect to the basis set in these systems, which also suggests that the cc-pVDZ basis set is too small for these systems and that basis sets with at least one augmenting set of basis functions give energies that are closer to convergence. Further, our choice of basis sets is constrained by the capabilities of Dalton's non-parallelized CC3 implementation of 2PA cross sections. Below, we discuss the results for the Dunning double zeta (aug-cc-pVDZ) basis set, which is a fairly large basis set for these prototypical polyenes. We restrict the discussion to the comparisons across different electronic structure methods and do not discuss whether the computed 2PA cross sections are converged with respect to the basis-set size. A more thorough discussion on the basis-set dependence of 2PA cross sections is given in Refs. 43 and 49.

For ethene's N → Z transition, the excitation energy with EOM-DEA-CCSD/aug-cc-pVDZ is underestimated by ~0.5 eV relative to that computed with the CC3 method, primarily a consequence of the differing dynamical correlation for the two methods and the unbalanced EOM-DEA-CCSD treatment of the singly excited configurations from the HOMO (VV) and from other occupied orbitals ($OVVV$), as explained in Sec. V A. Moreover, this transition corresponds to the $XA_g \rightarrow 3A_g$ within the EOM-DEA-CCSD framework,

TABLE IV. Vertical excitation energies in eV for the $1B_u$ and $2A_g$ states in butadiene, hexatriene, and octatetraene computed with the EOM-DEA-CCSD method for different basis sets.

	Butadiene		Hexatriene		Octatetraene	
Basis set	$1B_u$	$2A_g$	$1B_u$	$2A_g$	$1B_u$	$2A_g$
cc-pVDZ	6.89	7.41	5.73	6.16	4.99	5.23
aug-cc-pVDZ	6.27	6.68	5.36	5.89	4.73	5.09
aug-cc-pVTZ	6.24	6.68	5.35	5.88	-	-

TABLE V. Vertical excitation energies (Ω^{fg}) and 2PA cross sections (δ^{fg}) for the N → Z transition in ethene and $XA_g \rightarrow 2A_g$ transitions in butadiene, hexatriene, and octatetraene computed with the CC3 quadratic response theory, the EOM-DEA-CCSD expectation-value, and the EOM-EE-CCSD expectation-value approaches.

	CC3		EOM-DEA-CCSD		EOM-EE-CCSD	
Basis set	Ω^{fg} (eV)	δ^{fg} (a.u.)	Ω^{fg} (eV)	δ^{fg} (a.u.)	Ω^{fg} (eV)	δ^{fg} (a.u.)
			Ethene			
aug-cc-pVDZ	13.62	1643.2	13.08	1303.3	-	-
aug-cc-pVTZ	-	-	12.86	674.8	-	-
			Butadiene			
cc-pVDZ	6.97	135.2	7.41	22.8	7.65	579.2
aug-cc-pVDZ	6.66	400.3	6.68	319.3	7.06	1018.4
			Hexatriene			
cc-pVDZ	5.84	613.3	6.16	97.9	6.76	4632.7
aug-cc-pVDZ	5.72	1300.8	5.89	482.1	6.53	8540.3
			Octatetraene			
aug-cc-pVDZ	-	-	5.09	145.9	-	-

again as a result of EOM-DEA-CCSD overestimating the energies of low-lying excitations from occupied orbitals lower than the HOMO. Still, its 2PA cross section is expected to be well described with the EOM-DEA-CCSD method as the dominant configuration in the final state is doubly excited relative to the dominant configuration in the initial state, as explained in the 2PA channel analysis surrounding Table I. Indeed, the 2PA cross sections with the EOM-DEA-CCSD method differ by ~20% relative to those computed with the CC3 response theory method. This difference also results from a combination of the differing dynamical correlation and the use of the expectation-value approach with EOM-DEA-CCSD as against the full response CC3 approach.

Similar to the above transition in ethene, EOM-DEA-CCSD is expected to perform well for the $XA_g \rightarrow 2A_g$ transition in butadiene. As detailed in Ref. 39, the $2A_g$ state has a mixed Rydberg and doubly excited character. EOM-DEA-CCSD yields the energy for this excitation within 0.03 eV of that computed with the CC3 method, which highlights that EOM-DEA-CCSD is able to balance Rydberg and doubly excited determinants on an equal footing. Since the dominant configurations in the initial and final states differ by either singles or doubles excitations relative to each other, EOM-DEA-CCSD is also expected to perform well for computing the 2PA cross sections, similar to the case of ethene discussed earlier and consistent with the channel analysis in Tables I and II. In the case of butadiene, the EOM-DEA-CCSD underestimates the 2PA cross section by ~20% relative to the CC3 response theory value. Here, we also note that EOM-EE-CCSD overestimates this excitation energy by 0.4 eV and 2PA cross section by ~150%.

Besides the doubly excited character and excitations from the HOMO, the CC3 wave-function amplitudes of hexatriene's $2A_g$ state reveal a more significant contribution from excitations originating from the lower occupied orbitals compared to similar excitations in ethene and butadiene. Since these excitations in the CC3 framework correspond to the *OVVV* configurations in EOM-DEA-CCSD, the corresponding *OVVV* amplitudes of the EOM-DEA-CCSD target state are negligible. Therefore, we expect EOM-DEA-CCSD to not perform well for the energy and 2PA cross section of the $XA_g \rightarrow 2A_g$ transition in hexatriene. Indeed, the discrepancy in the excitation energy of this state between CC3 and EOM-DEA-CCSD (0.14 eV) is larger than that in butadiene. Although the impact of this unbalanced EOM-DEA-CCSD description of the final state is not considerable in the excitation energy, the impact on the 2PA cross section is much larger. The EOM-DEA-CCSD yields a 2PA cross section for hexatriene's $XA_g \rightarrow 2A_g$ transition that is smaller by a factor of ~2.5 compared to the value computed with the CC3 response theory. Finally, as expected, EOM-EE-CCSD performs even worse than EOM-DEA-CCSD for both the excitation energy and the 2PA cross section for this transition; the excitation energy is overestimated by ~0.7 eV and the 2PA cross section is overestimated by a factor of ~7.

Finally, we do not see a monotonous trend in the 2PA cross sections with increasing length of polyenes. Instead, the EOM-DEA-CCSD 2PA cross sections oscillate from ethene to octatetraene, following a similar trend observed for the CC3 quadratic response theory approach.

VI. CONCLUSIONS

We expanded the scope of the EOM-CC framework to include the calculations of 2PA cross sections for transitions between EOM-DEA-CCSD target states. To derive the working equations, we began with the SOS expressions for the 2PA transition moments, derived from time-dependent perturbation theory for exact states, and parameterized them with EOM-DEA-CCSD energies and wave functions. We then recast the SOS expression to a more compact

expectation-value-like form using first-order response wave functions. These response wave functions are computed by solving systems of linear equations, which have the same computational complexity as the EOM-DEA-CCSD eigenproblem. We benchmarked the 2PA cross sections for one-photon dark transitions in prototypical polyenes and twisted ethene computed with this EOM-DEA-CCSD approach against the ones computed with the higher-level CC3 quadratic response theory. We showed that the results for 2PA cross sections for transitions to target states dominated by the doubly excited character in twisted ethene were of similar quality for the EOM-DEA-CCSD and CC3 approaches, whereas the EOM-EE-CCSD method showed large errors relative to CC3, as expected. In contrast, the 2PA cross sections for $XA_g \rightarrow 2A_g$ transitions in polyenes showed larger discrepancies between the CC3 and EOM-DEA-CCSD methods, even though the EOM-DEA-CCSD method gives energies and zero-order wave functions of these target states with significant multiconfigurational character that are of similar quality as CC3. By using a simplified representation of 2PA configurational channels, we explained that these discrepancies arise mostly when the CC3 wave functions of the initial or final target states have a non-negligible contribution from configurations that involve excitations from occupied orbitals other than the HOMO. Because EOM-DEA-CCSD does not have sufficient dynamical correlation (i.e., from the triples) to reliably describe these configurations, which are of the type *OVVV* in EOM-DEA-CCSD target wave functions, 2PA cross sections, which are strongly sensitive to electronic correlation through the SOS expressions, showed larger discrepancies compared to the discrepancies in the state energies. We conclude that non-particle-conserving flavors of EOM-CCSD, such as EOM-DEA-CCSD $(2p + 3p1h)$ and other similar multireference methods, which can provide reliable energies and first-order properties for systems such as polyenes and diradicals by exploiting specific sectors of the Fock space and the choice of the reference(s), might not be reliable for multiphoton properties. On the other hand, computationally more demanding methods such as EOM-DEA-CCSD with $2p + 3p1h + 4p2h$ DEA operators and EOM-nEA-CC (n = T, Q, ...) can potentially deliver accurate results for specific multiphoton transitions in these systems, and will be explored in the future studies.

SUPPLEMENTARY MATERIAL

See the supplementary material for the Cartesian coordinates of the benchmark systems.

ACKNOWLEDGMENTS

This work was supported by the U.S. National Science Foundation (Grant No. CHE-2154482 to A.I.K.). We are grateful to Professor Sonia Coriani from DTU, Lingby, for her help with the CC3 calculations for hexatriene.

AUTHOR DECLARATIONS

Conflict of Interest

A.I.K. is the president and a part-owner of Q-Chem, Inc.

Author Contributions

Kaushik D. Nanda: Conceptualization (lead); Data curation (lead); Formal analysis (lead); Investigation (lead); Methodology (lead); Software (lead); Supervision (equal); Validation (equal); Writing – original draft (lead); Writing – review & editing (lead). **Sahil Gulania**: Formal analysis (supporting); Methodology (supporting); Software (supporting); Validation (equal); Writing – original draft (supporting); Writing – review & editing (supporting). **Anna I. Krylov**: Data curation (supporting); Funding acquisition (lead); Project administration (lead); Resources (lead); Supervision (equal); Writing – original draft (equal); Writing – review & editing (equal).

DATA AVAILABILITY

The data that support the findings of this study are available within the article and its supplementary material.

APPENDIX: 2PA RESPONSE INTERMEDIATES AND MO PICTURE OF THE N → Z TRANSITION IN TWISTED ETHENE

1. Programmable expressions

Below, $\mathscr{P}^-_{ab}$ denotes the anti-symmetrizer with respect to indices a and b; $\mathscr{P}^-_{abc}$ denotes the anti-symmetrizer with respect to indices a, b, and c; and $\mathrm{tr}(A)$ denotes the trace of tensor A:

$$D^{ab} = \mathscr{P}^-_{ab}\sum_c \mu^{ac} r^{cb} + \mathrm{tr}(\mu_{ij}) r^{ab} + r^{ab}\left(\sum_{ie} \mu_i^e t_i^e\right) - \mathscr{P}^-_{ab}\sum_i \left(\sum_c \mu_i^c r^{ac}\right) t_i^b + \sum_{ic} \mu_i^c r_i^{abc}, \tag{A1}$$

$$\begin{aligned} D_i^{abc} = 0.5\mathscr{P}^-_{abc}\Bigg(& \mu_i^c r^{ab} + \sum_e \mu^{ae} t_i^e r^{bc} - \sum_j \mu_{ji} t_j^c r^{ab} \\ & + \sum_j \left(\sum_e \mu_j^e r^{ce}\right) t_{ij}^{ab} + \sum_{je} \mu_j^e t_{ij}^{ce} r^{ab} - r^{ab}\sum_j \left(\sum_e \mu_j^e t_i^e\right) t_j^c \\ & + \sum_e \mu^{ae} r_i^{bce} - \sum_j \sum_e \left(\mu_j^e r_i^{abe}\right) t_j^c \Bigg) - \sum_j \mu_{ji} r_j^{abc} \\ & + \mathrm{tr}(\mu_{kj}) r_i^{abc} + \left(\sum_{je} \mu_j^e t_j^e\right) r_i^{abc} - \sum_j \left(\sum_e \mu_j^e t_i^e\right) r_j^{abc}, \end{aligned} \tag{A2}$$

$$\begin{aligned} \tilde{D}^{ab} = \mathscr{P}^-_{ab}\Bigg(& \sum_c l^{ac}\mu^{cb} - \sum_i \left(\sum_c l^{ac} t_i^c\right)\mu_i^b \\ & + 0.5\sum_j \left(\sum_{icd} l_i^{acd} t_{ij}^{cd}\right)\mu_j^b \Bigg) + l^{ab}\,\mathrm{tr}(\mu_{ij}) + l^{ab}\sum_{je}\left(\mu_i^c t_i^c\right) \\ & + \sum_{ic} l_i^{abc}\left(\sum_d \mu^{cd} t_i^d\right) + \sum_{ic} l_i^{abc}\mu_i^c - \sum_{ic} l_i^{abc}\sum_j \left(t_j^c \sum_d \left(t_i^d \mu_j^d\right)\right) \\ & + \sum_{ic} l_i^{abc}\left(\sum_{jd} \mu_j^d t_{ij}^{cd}\right) - \sum_{ic} l_i^{abc}\left(\sum_j \mu_{ji} t_j^c\right), \end{aligned} \tag{A3}$$

$$\tilde{D}_i^{abc} = 0.5\bar{\mathscr{P}}_{abc}\left(l^{ab}\mu_i^c + \sum_e l_i^{abe}\mu^{ec} - \sum_j\left(\sum_e l_i^{abe}t_j^e\right)\mu_j^c\right) - \sum_j l_j^{abc}\left(\sum_e \mu_i^e t_j^e\right) - \sum_j l_j^{abc}\mu_{ij} + l_j^{abc}\sum_{je}\left(\mu_j^e t_j^e\right) + \; l_j^{abc}\,\mathrm{tr}(\mu_{kj}). \tag{A4}$$

2. Why $\langle\Psi_N|\mu|\Psi_V\rangle$ decreases to zero for perfectly twisted ethene?

We consider the simple two-electrons-in-two-molecular-orbitals picture such that the wave functions, Ψ_N and Ψ_V, of the N and V states, respectively, are given by

$$\Psi_N = \frac{\left(\cos(\theta)\phi_1^2 - \sin(\theta)\phi_2^2\right)(\alpha\beta - \beta\alpha)}{2} \tag{A5}$$

and

$$\Psi_V = \frac{(\phi_1\phi_2 + \phi_2\phi_1)(\alpha\beta - \beta\alpha)}{2}, \tag{A6}$$

where ϕ_1 and ϕ_2 are the two frontier MOs forming the bonding–antibonding MO pair from two atomic orbitals χ_a and χ_b, each on the two carbon atoms a and b, such that

$$\phi_1 = \frac{\chi_a + \chi_b}{\sqrt{2}} \tag{A7}$$

and

$$\phi_2 = \frac{\chi_a - \chi_b}{\sqrt{2}}. \tag{A8}$$

Here, α and β indicate the electron spins and 2θ is the torsion angle. The above wave functions can also be expressed in terms of λ, which is an indicator of the diradical character of ethene, as in Ref. 60. λ depends on the energy separation of the two MOs and is related to θ via $\lambda = \tan(\theta)$. $\lambda = 1$ when these MOs are degenerate, which is the case for perfectly twisted ethene. The dipole coupling between these two wave functions is given by

$$\begin{aligned}\langle\Psi_N|\mu|\Psi_V\rangle &= \frac{1}{4}\langle\left(\cos(\theta)\phi_1^2 - \sin(\theta)\phi_2^2\right)|\mu|(\phi_1\phi_2 + \phi_2\phi_1)\rangle \\ &= \frac{1}{2}(\cos(\theta) - \sin(\theta))\langle\phi_1|\mu|\phi_2\rangle \\ &= \frac{1}{2\sqrt{1+\lambda^2}}(1-\lambda)\langle\phi_1|\mu|\phi_2\rangle,\end{aligned} \tag{A9}$$

where we use $\langle\phi_1|\mu|\phi_2\rangle = \langle\phi_2|\mu|\phi_1\rangle$. Inserting Eqs. (A7) and (A8) in Eq. (A9), we obtain

$$\begin{aligned}\langle\Psi_N|\mu|\Psi_V\rangle &= \frac{1}{2\sqrt{1+\lambda^2}}(1-\lambda)\langle\frac{\chi_a + \chi_b}{\sqrt{2}}|\mu|\frac{\chi_a - \chi_b}{\sqrt{2}}\rangle \\ &\approx \frac{1}{4\sqrt{1+\lambda^2}}(1-\lambda)(\langle\chi_a|\mu|\chi_a\rangle - \langle\chi_b|\mu|\chi_b\rangle) \\ &\approx \frac{1}{4\sqrt{1+\lambda^2}}(1-\lambda)(r_b - r_a).\end{aligned} \tag{A10}$$

Because λ increases to 1 for perfectly twisted ethene, the above term drops to zero, thereby, making the M_{xx}^{NZ} 2PA moments negligible.

REFERENCES

[1] E. C. Carroll, S. Berlin, J. Levitz, M. A. Kienzler, Z. Yuan, D. Madsen, D. S. Larsen, and E. Y. Isacoff, "Two-photon brightness of azobenzene photoswitches designed for glutamate receptor optogenetics," Proc. Natl. Acad. Sci. U. S. A. **112**, E776 (2015).

[2] M. Nakano, R. Kishi, S. Ohta, H. Takahashi, T. Kubo, K. Kamada, K. Ohta, E. Botek, and B. Champagne, "Relationship between third-order nonlinear optical properties and magnetic interactions in open-shell systems: A new paradigm for nonlinear optics," Phys. Rev. Lett. **99**, 033001 (2007).

[3] Y. Li, W.-K. Heng, B. S. Lee, N. Aratani, J. L. Zafra, N. Bao, R. Lee, Y. M. Sung, Z. Sun, K.-W. Huang, R. D. Webster, J. T. López Navarrete, D. Kim, A. Osuka, J. Casado, J. Ding, and J. Wu, "Kinetically blocked stable heptazethrene and octazethrene: Closed-shell or open-shell in the ground state?," J. Am. Chem. Soc. **134**, 14913 (2012).

[4] M. Nakano and B. Champagne, "Nonlinear optical properties in open-shell molecular systems," WIREs: Comput. Mol. Sci. **6**, 198 (2016).

[5] G. S. He, J. Zhu, A. Baev, M. Samoć, D. L. Frattarelli, N. Watanabe, A. Facchetti, H. Ågren, T. J. Marks, and P. N. Prasad, "Twisted π-system chromophores for all-optical switching," J. Am. Chem. Soc. **133**, 6675 (2011).

[6] S. K. Pati, T. J. Marks, and M. A. Ratner, "Conformationally tuned large two-photon absorption cross sections in simple molecular chromophores," J. Am. Chem. Soc. **123**, 7287 (2001).

[7] J. D. Bhawalkar, G. S. He, and P. N. Prasad, "Nonlinear multiphoton processes in organic and polymeric materials," Rep. Prog. Phys. **59**, 1041 (1996).

[8] M. Marazzi, C. García-Iriepa, C. Benitez-Martin, F. Najera, A. Monari, and D. Sampedro, "*E/Z* molecular photoswitches activated by two-photon absorption: Comparison between different families," Molecules **26**, 7379 (2021).

[9] S. Shih, R. J. Buenker, and S. D. Peyerimhoff, "Non-empirical calculations on the electronic spectrum of butadiene," Chem. Phys. Lett. **16**, 244 (1972).

[10] J. P. Doering and R. McDiarmid, "100 eV electron impact study of 1,3-butadiene," J. Chem. Phys. **75**, 2477 (1981).

[11] J. H. Starcke, M. Wormit, J. Schirmer, and A. Dreuw, "How much double excitation character do the lowest excited states of linear polyenes have?," Chem. Phys. **329**, 39 (2006).

[12] G. Mazur and R. Włodarczyk, "Application of the dressed time-dependent density functional theory for the excited states of linear polyenes," J. Comput. Chem. **30**, 811 (2009).

[13] M. Schmidt and P. Tavan, "Electronic excitations in long polyenes revisited," J. Chem. Phys. **136**, 124309 (2012).

[14] M. A. Watson and G. K.-L. Chan, "Excited states of butadiene to chemical accuracy: Reconciling theory and experiment," J. Chem. Theory Comput. **8**, 4013 (2012).

[15] J. D. Watts, S. R. Gwaltney, and R. J. Bartlett, "Coupled-cluster calculations of the excitation energies of ethylene, butadiene, and cyclopentadiene," J. Chem. Phys. **105**, 6979 (1996).

[16] A. D. Chien, A. A. Holmes, M. Otten, C. J. Umrigar, S. Sharma, and P. M. Zimmerman, "Excited states of methylene, polyenes, and ozone from heat-bath configuration interaction," J. Phys. Chem. A **122**, 2714 (2018).

[17] S. Manna, R. K. Chaudhuri, and S. Chattopadhyay, "Taming the excited states of butadiene, hexatriene, and octatetraene using state specific multireference perturbation theory with density functional theory orbitals," J. Chem. Phys. **152**, 244105 (2020).

[18] P. M. Zimmerman, "Incremental full configuration interaction," J. Chem. Phys. **146**, 104102 (2017).

[19] P. M. Zimmerman, "Singlet–triplet gaps through incremental full configuration interaction," J. Phys. Chem. A **121**, 4712 (2017).

[20] K. Emrich, "An extension of the coupled-cluster formalism to excited states (I)," Nucl. Phys. A **351**, 379 (1981).

[21] H. Sekino and R. J. Bartlett, "A linear response, coupled-cluster theory for excitation energy," Int. J. Quantum Chem. **26**, 255 (1984).

[22] H. Koch and P. Jørgensen, "Coupled cluster response functions," J. Chem. Phys. **93**, 3333 (1990).

[23] H. Koch, H. J. r. A. Jensen, P. Jørgensen, and T. Helgaker, "Excitation energies from the coupled clusters singles and doubles linear response functions

(CCSDLR). Applications to Be, CH^+, CO, and H_2O," J. Chem. Phys. **93**, 3345 (1990).
[24]J. F. Stanton and R. J. Bartlett, "The equation of motion coupled-cluster method. A systematic biorthogonal approach to molecular excitation energies, transition probabilities, and excited state properties," J. Chem. Phys. **98**, 7029 (1993).
[25]M. Nooijen and R. J. Bartlett, "Description of core-excitation spectra by the open-shell electron-attachment equation-of-motion coupled cluster method," J. Chem. Phys. **102**, 6735 (1995).
[26]S. V. Levchenko and A. I. Krylov, "Equation-of-motion spin-flip coupled-cluster model with single and double substitutions: Theory and application to cyclobutadiene," J. Chem. Phys. **120**, 175 (2004).
[27]A. I. Krylov, "Equation-of-motion coupled-cluster methods for open-shell and electronically excited species: The hitchhiker's guide to Fock space," Annu. Rev. Phys. Chem. **59**, 433 (2008).
[28]K. Sneskov and O. Christiansen, "Excited state coupled cluster methods," WIREs: Comput. Mol. Sci. **2**, 566 (2012).
[29]R. J. Bartlett, "Coupled-cluster theory and its equation-of-motion extensions," WIREs: Comput. Mol. Sci. **2**, 126 (2012).
[30]A. I. Krylov, "The quantum chemistry of open-shell species", in *Reviews in Computational Chemistry*, edited by A. L. Parrill and K. B. Lipkowitz (J. Wiley & Sons, 2017), Vol. 30, pp. 151–224.
[31]A. I. Krylov, "Size-consistent wave functions for bond-breaking: The equation-of-motion spin-flip model," Chem. Phys. Lett. **338**, 375 (2001).
[32]D. Casanova and A. I. Krylov, "Spin-flip methods in quantum chemistry," Phys. Chem. Chem. Phys. **22**, 4326 (2020).
[33]K. W. Sattelmeyer, H. F. Schaefer III, and J. F. Stanton, "Use of 2h and 3h-p like coupled-cluster Tamm-Dancoff approaches for the equilibrium properties of ozone," Chem. Phys. Lett. **378**, 42 (2003).
[34]M. Musiaz, S. A. Kucharski, and R. J. Bartlett, "Multireference double electron attached coupled cluster method with full inclusion of the connected triple excitations: MR-DA-CCSDT," J. Chem. Theory Comput. **7**, 3088 (2011).
[35]J. Shen and P. Piecuch, "Doubly electron-attached and doubly ionized equation-of-motion coupled-cluster methods with 4-particle-2-hole and 4-hole-2-particle excitations and their active-space extensions," J. Chem. Phys. **138**, 194102 (2013).
[36]M. Nooijen and R. J. Bartlett, "Similarity transformed equation-of-motion coupled-cluster theory: Details, examples, and comparisons," J. Chem. Phys. **107**, 6812 (1997).
[37]D. Bokhan, D. N. Trubnikov, A. Perera, and R. J. Bartlett, "Explicitly-correlated double ionization potentials and double electron attachment equation-of-motion coupled cluster methods," Chem. Phys. Lett. **692**, 191 (2018).
[38]A. Perera, R. W. Molt, V. F. Lotrich, and R. J. Bartlett, "Singlet-triplet separations of di-radicals treated by the DEA/DIP-EOM-CCSD methods," in *Isaiah Shavitt: A Memorial Festschrift from Theoretical Chemistry Accounts*, edited by C. J. Cramer and D. G. Truhlar (Springer, 2016), Vol. 9, pp. 153–165.
[39]S. Gulania, E. F. Kjønstad, J. F. Stanton, H. Koch, and A. I. Krylov, "Equation-of-motion coupled-cluster method with double electron-attaching operators: Theory, implementation, and benchmarks," J. Chem. Phys. **154**, 114115 (2021).
[40]H. Koch, O. Christiansen, P. Jørgensen, and J. Olsen, "Excitation energies of BH, CH_2, and Ne in full configuration interaction and the hierarchy CCS, CC2, CCSD, and CC3 of coupled cluster models," Chem. Phys. Lett. **244**, 75 (1995).
[41]H. Koch, O. Christiansen, P. Jørgensen, A. M. Sanchez de Merás, and T. Helgaker, "The CC3 model: An iterative coupled cluster approach including connected triples," J. Chem. Phys. **106**, 1808 (1997).
[42]O. Christiansen, H. Koch, and P. Jørgensen, "Response functions in the CC3 iterative triple excitation model," J. Chem. Phys. **103**, 7429 (1995).
[43]M. J. Paterson, O. Christiansen, F. Pawłowski, P. Jorgensen, C. Hättig, T. Helgaker, and P. Sałek, "Benchmarking two-photon absorption with CC3 quadratic response theory, and comparison with density-functional response theory," J. Chem. Phys. **124**, 054322 (2006).
[44]H. J. Monkhorst, "Calculation of properties with the coupled-cluster method," Int. J. Quant. Chem. Symp. **12**, 421–432 (1977).
[45]S. V. Levchenko, T. Wang, and A. I. Krylov "Analytic gradients for the spin-conserving and spin-flipping equation-of-motion coupled-cluster models with single and double substitutions," J. Chem. Phys. **122**, 224106 (2005).
[46]R. J. Bartlett, "How and why coupled-cluster theory became the preeminent method in *ab initio* quantum chemistry," in *Theory and Applications of Computational Chemistry*, edited by C. Dykstra, G. Frenking and G. Scuseria (Elsevier, 2005).
[47]I. Shavitt and R. J. Bartlett, *Many-Body Methods in Chemistry and Physics: MBPT and Coupled-Cluster Theory* (Cambridge University Press, Cambridge, 2009).
[48]R. J. Bartlett, "The coupled-cluster revolution," Mol. Phys. **108**, 2905 (2010).
[49]K. D. Nanda and A. I. Krylov, "Two-photon absorption cross sections within equation-of-motion coupled-cluster formalism using resolution-of-the-identity and Cholesky decomposition representations: Theory, implementation, and benchmarks," J. Chem. Phys. **142**, 064118 (2015).
[50]C. Hättig, O. Christiansen, and P. Jørgensen, "Multiphoton transition moments and absorption cross sections in coupled cluster response theory employing variational transition moment functionals," J. Chem. Phys. **108**, 8331 (1998).
[51]T. Helgaker, S. Coriani, P. Jørgensen, K. Kristensen, J. Olsen, and K. Ruud, "Recent advances in wave function-based methods of molecular-property calculations," Chem. Rev. **112**, 543 (2012).
[52]O. Christiansen, A. Halkier, H. Koch, P. Jørgensen, and T. Helgaker, "Integral-direct coupled cluster calculations of frequency-dependent polarizabilities, transition probabilities and excited-state properties," J. Chem. Phys. **108**, 2801 (1998).
[53]C. Hättig and P. Jørgensen, "Derivation of coupled cluster excited states response functions and multiphoton transition moments between two excited states as derivatives of variational functinals," J. Chem. Phys. **109**, 9219 (1998).
[54]K. D. Nanda and A. I. Krylov, "Static polarizabilities for excited states within the spin-conserving and spin-flipping equation-of-motion coupled-cluster singles and doubles formalism: Theory, implementation, and benchmarks," J. Chem. Phys. **145**, 204116 (2016).
[55]K. D. Nanda, A. I. Krylov, and J. Gauss, "Communication: The pole structure of the dynamical polarizability tensor in equation-of-motion coupled-cluster theory," J. Chem. Phys. **149**, 141101 (2018).
[56]K. D. Nanda, M. L. Vidal, R. Faber, S. Coriani, and A. I. Krylov, "How to stay out of trouble in RIXS calculations within the equation-of-motion coupled-cluster damped response theory framework? Safe hitchhiking in the excitation manifold by means of core-valence separation," Phys. Chem. Chem. Phys. **22**, 2629 (2020).
[57]K. D. Nanda and A. I. Krylov, "The orbital picture of the first dipole hyperpolarizability from many-body response theory," J. Chem. Phys. **154**, 184109 (2021).
[58]J. H. Andersen, K. D. Nanda, A. I. Krylov, and S. Coriani, "Cherry-picking resolvents: Recovering the valence contribution in x-ray two-photon absorption within the core-valence-separated equation-of-motion coupled-cluster response theory," J. Chem. Theory Comput. **18**, 6189 (2022).
[59]E. Epifanovsky, A. T. B. Gilbert, X. Feng, J. Lee, Y. Mao, N. Mardirossian, P. Pokhilko, A. F. White, M. P. Coons, A. L. Dempwolff, Z. Gan, D. Hait, P. R. Horn, L. D. Jacobson, I. Kaliman, J. Kussmann, A. W. Lange, K. U. Lao, D. S. Levine, J. Liu, S. C. McKenzie, A. F. Morrison, K. D. Nanda, F. Plasser, D. R. Rehn, M. L. Vidal, Z.-Q. You, Y. Zhu, B. Alam, B. J. Albrecht, A. Aldossary, E. Alguire, J. H. Andersen, V. Athavale, D. Barton, K. Begam, A. Behn, N. Bellonzi, Y. A. Bernard, E. J. Berquist, H. G. A. Burton, A. Carreras, K. Carter-Fenk, R. Chakraborty, A. D. Chien, K. D. Closser, V. Cofer-Shabica, S. Dasgupta, M. de Wergifosse, J. Deng, M. Diedenhofen, H. Do, S. Ehlert, P.-T. Fang, S. Fatehi, Q. Feng, T. Friedhoff, J. Gayvert, Q. Ge, G. Gidofalvi, M. Goldey, J. Gomes, C. E. González-Espinoza, S. Gulania, A. O. Gunina, M. W. D. Hanson-Heine, P. H. P. Harbach, A. Hauser, M. F. Herbst, M. Hernández Vera, M. Hodecker, Z. C. Holden, S. Houck, X. Huang, K. Hui, B. C. Huynh, M. Ivanov, Á. Jász, H. Ji, H. Jiang, B. Kaduk, S. Kähler, K. Khistyaev, J. Kim, G. Kis, P. Klunzinger, Z. Koczor-Benda, J. H. Koh, D. Kosenkov, L. Koulias, T. Kowalczyk, C. M. Krauter, K. Kue, A. Kunitsa, T. Kus, I. Ladjánszki, A. Landau, K. V. Lawler, D. Lefrancois, S. Lehtola, R. R. Li, Y.-P. Li, J. Liang, M. Liebenthal, H.-H. Lin, Y.-S. Lin, F. Liu, K.-Y. Liu, M. Loipersberger, A. Luenser, A. Manjanath, P. Manohar, E. Mansoor, S. F. Manzer, S.-P. Mao, A. V. Marenich, T. Markovich, S. Mason, S. A. Maurer, P. F. McLaughlin, M. F. S. J. Menger, J.-M. Mewes, S. A. Mewes, P. Morgante, J. W. Mullinax, K. J. Oosterbaan, G. Paran, A. C. Paul, S. K. Paul, F. Pavošević, Z. Pei, S. Prager, E. I. Proynov, Á. Rák, E. Ramos-Cordoba, B. Rana, A. E. Rask, A. Rettig, R. M. Richard, F. Rob, E. Rossomme, T. Scheele, M. Scheurer, M. Schneider, N. Sergueev, S. M. Sharada, W. Skomorowski,

D. W. Small, C. J. Stein, Y.-C. Su, E. J. Sundstrom, Z. Tao, J. Thirman, G. J. Tornai, T. Tsuchimochi, N. M. Tubman, S. P. Veccham, O. Vydrov, J. Wenzel, J. Witte, A. Yamada, K. Yao, S. Yeganeh, S. R. Yost, A. Zech, I. Y. Zhang, X. Zhang, Y. Zhang, D. Zuev, A. Aspuru-Guzik, A. T. Bell, N. A. Besley, K. B. Bravaya, B. R. Brooks, D. Casanova, J.-D. Chai, S. Coriani, C. J. Cramer, G. Cserey, A. E. DePrince, R. A. DiStasio, A. Dreuw, B. D. Dunietz, T. R. Furlani, W. A. Goddard, S. Hammes-Schiffer, T. Head-Gordon, W. J. Hehre, C.-P. Hsu, T.-C. Jagau, Y. Jung, A. Klamt, J. Kong, D. S. Lambrecht, W. Liang, N. J. Mayhall, C. W. McCurdy, J. B. Neaton, C. Ochsenfeld, J. A. Parkhill, R. Peverati, V. A. Rassolov, Y. Shao, L. V. Slipchenko, T. Stauch, R. P. Steele, J. E. Subotnik, A. J. W. Thom, A. Tkatchenko, D. G. Truhlar, T. Van Voorhis, T. A. Wesolowski, K. B. Whaley, H. L. Woodcock, P. M. Zimmerman, S. Faraji, P. M. W. Gill, M. Head-Gordon, J. M. Herbert, and A. I. Krylov, "Software for the frontiers of quantum chemistry: An overview of developments in the Q-Chem 5 package," J. Chem. Phys. **155**, 084801 (2021).

[60] K. D. Nanda and A. I. Krylov, "Effect of the diradical character on static polarizabilities and two-photon absorption cross-sections: A closer look with spin-flip equation-of-motion coupled-cluster singles and doubles method," J. Chem. Phys. **146**, 224103 (2017).

[61] K. D. Nanda and A. I. Krylov, "Visualizing the contributions of virtual states to two-photon absorption cross-sections by natural transition orbitals of response transition density matrices," J. Phys. Chem. Lett. **8**, 3256 (2017).

[62] K. Aidas, C. Angeli, K. L. Bak, V. Bakken, R. Bast, L. Boman, O. Christiansen, R. Cimiraglia, S. Coriani, P. Dahle, E. K. Dalskov, U. Ekström, T. Enevoldsen, J. J. Eriksen, P. Ettenhuber, B. Fernández, L. Ferrighi, H. Fliegl, L. Frediani, K. Hald, A. Halkier, C. Hättig, H. Heiberg, T. Helgaker, A. C. Hennum, H. Hettema, E. Hjertenaes, S. Høst, I.-M. Høyvik, M. F. Iozzi, B. Jansík, H. J. A. Jensen, D. Jonsson, P. Jørgensen, J. Kauczor, S. Kirpekar, T. Kjaergaard, W. Klopper, S. Knecht, R. Kobayashi, H. Koch, J. Kongsted, A. Krapp, K. Kristensen, A. Ligabue, O. B. Lutnaes, J. I. Melo, K. V. Mikkelsen, R. H. Myhre, C. Neiss, C. B. Nielsen, P. Norman, J. Olsen, J. M. H. Olsen, A. Osted, M. J. Packer, F. Pawlowski, T. B. Pedersen, P. F. Provasi, S. Reine, Z. Rinkevicius, T. A. Ruden, K. Ruud, V. V. Rybkin, P. Sałek, C. C. M. Samson, A. S. de Merás, T. Saue, S. P. A. Sauer, B. Schimmelpfennig, K. Sneskov, A. H. Steindal, K. O. Sylvester-Hvid, P. R. Taylor, A. M. Teale, E. I. Tellgren, D. P. Tew, A. J. Thorvaldsen, L. Thøgersen, O. Vahtras, M. A. Watson, D. J. D. Wilson, M. Ziolkowski, and H. Ågren, "The Dalton quantum chemistry program system," WIREs: Comput. Mol. Sci. **4**, 269 (2014).

[63] Dalton, a molecular electronic structure program, Release Dalton2020.0 (2020), see http://daltonprogram.org.

[64] Depending on molecular orientation, symmetry labels corresponding to the same orbital or vibrational mode may be different. Q-Chem's standard molecular orientation is different from that of Mulliken.[65] For example, Q-Chem places water molecule in xz-plane instead of yz. Consequently, for C_{2v} symmetry, b_1 and b_2 labels are flipped. More details can be found at http://iopenshell.usc.edu/resources/howto/symmetry.

[65] R. S. Mulliken, "Report on notation for the spectra of polyatomic molecules," J. Chem. Phys. **23**, 1997 (1955).

[66] W. Moffitt and J. Scanlan, "Some calculations on the ethylene molecule," Proc. R. Soc. London, Ser. A **218**, 464 (1953).

[67] H. Koch, R. Kobayashi, A. Sanchez de Merás, and P. Jørgensen, "Calculation of size-extensive transition moments from coupled cluster singles and doubles linear response function," J. Chem. Phys. **100**, 4393 (1994).